CHAPTER 13 - CHEMICAL ASPECTS OF LEACHING

The intent of this chapter is to:

(1) Use a classical geochemical approach to understanding leaching.
(2) Provide the fundamentals necessary to design and use appropriate leaching tests.
(3) Mechanistically evaluate the leaching data.
(4) Accurately model the leaching phenomena.

Where appropriate, mention is made in the text to references in the literature that provide more detailed information on the concepts that are presented.

13.1 LEACHING CHEMISTRY FUNDAMENTALS

The information presented here draws on research that has been conducted in the areas of aquatic chemistry, terrestrial geochemistry, marine aqueous chemistry, sediment biogeochemistry, and coal ash leaching. Reference is made as to how these systems are similar to MSW residue leaching systems. The reader may wish to delve further into these subjects. Useful texts or monographs include the following: for aquatic chemistry principles, Butler (1964), Pankow (1991) and Stumm and Morgan (1981); for geochemistry principles, Lindsay (1979), Sposito (1981, 1989), Drever (1988), Garrels and Christ (1965), Pytkowicz (1983), and Nordstrom and Munoz (1986); and for coal ash leaching, the work of de Groot et al. (1987) and various monographs produced by the Electric Power Research Institute (Rai and Zachara, 1984; Rai, 1987; Krupka et al., 1988; Zachara and Streile, 1991).

Throughout this chapter, the nomenclature of Pankow (1991) is generally used, as shown in Table 13.1. Activities are denoted as { } and concentration as [ ]. Generally, "M" stands for metal cation, "S" for base salt, "H" for proton, "OH" for hydroxyl, "A" for conjugate base of an acid and "L" for ligand.

13.1.1 Thermodynamic Equilibrium Models Versus Kinetic Models

The ability to understand leaching processes, utilise leach tests, interpret the data and ultimately model leaching requires an understanding of reaction kinetics. All leaching processes involve chemical reactions (Figure 13.1). Homogeneous reactions are those that take place in a single phase (e.g. solution complexation reactions). Heterogeneous reactions are those that take place in the presence of at least two phases (e.g. a solution containing a solid phase). Ash leaching systems are heterogeneous systems.

Table 13.1
Nomenclature

Example Reactions	Thermodynamic Parameters	Names	Common Units
• GAS PHASE			
	p_i, p_j, pk,...	partial pressures	atmospheres
$2H_2 + O_2 = 2H_2O$	$\gamma_{i,g}$, $\gamma_{j,g}$, $\gamma_{k,g}$,...	activity coefficients	dimensionless
	f_i, f_j, f_k,...	fugacities	atmospheres
• AQUEOUS PHASE			
	[i], [j], [k],...	concentrations	mol/L (M) or mol/kg (m)
$H_2CO_3 = HCO_3^- + H^+$	γ_i, γ_j, γ_k,...	activity coefficients	dimensionless
	{i}, {j}, {k},...	activities	mol/L (M) or mol/kg (m)

Figure 13.1 Chemical Reactions

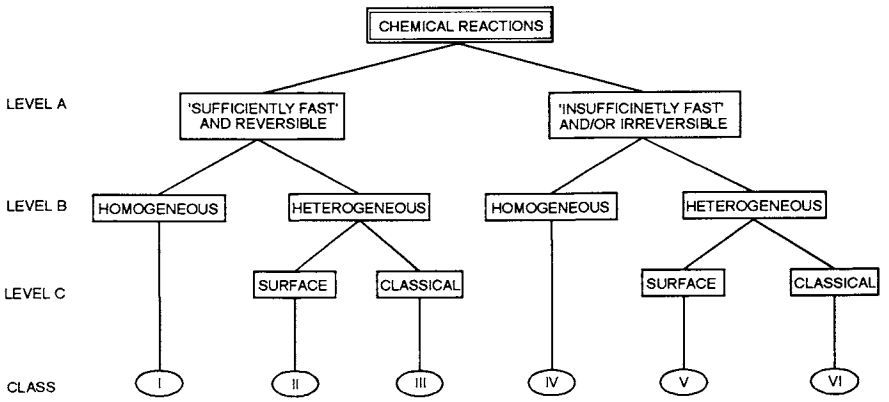

Adapted from Rubin, 1983 with permission, copyright by the American Geophysical Union

Most chemical reactions are reversible, but some are relatively fast and others relatively slow. It is important to understand the specific time frame under which these reactions occur, i.e., from fractions of a second to millennia. Aqueous phase reactions such as acid-base reactions or complexation reactions are usually fast, in the order of fractions of a second to a few seconds (Stumm and Morgan, 1981). Surface sorption reactions such as lead or cadmium adsorbing to oxide surfaces are in the order of hours to days (Cole, 1983). Precipitation, dissolution, and redox reactions involving solid phases are slow, in the order of hours to years (Stumm and Morgan, 1981).

Diagenetic changes in crystal structure and mineral predominance and weathering reactions are very slow, in the order of months to millennia (Berner, 1981). In contrast, some leaching tests vary in their time frame from hours, to days, to weeks and occasionally years. Clearly, the time frame of the leaching scenario will dictate the type of reactions that can be observed.

Figure 13.2 shows the change in solute concentration of Al, Ca and OH extracted from bottom ash from a Swiss incinerator by mixing the ash in a closed system. The reactions are heterogeneous in that a solution phase and a solid phase are both present. Initially, aluminum is inclined to dissolve from the solid phase and go into solution; however, the system is not yet in equilibrium. Further, calcium ions and hydroxide ions are inclined to precipitate out of solution until the solid is in equilibrium with the solution concentration of these components. As these reactions progress, high concentrations of hydroxide and calcium decrease to a constant equilibrium value (5.6 mm) while aluminum concentrations increase to a constant equilibrium value (5 to 6 mm) by about 10 to 100 hours. In the time frame of the observer, the equilibrium between the solution and the solid phase under the conditions of the system could be viewed as both fast (hours) and reversible (some reprecipitation is occurring at equilibrium). Consequently, if a leaching experiment or leaching test were designed to evaluate the equilibrium relations of calcium, hydroxide and aluminum with a bottom ash solid phase, and the time frame was greater than 10 to 100 hours, then the system could be said to be governed by fast, reversible reactions and that this condition could be described using thermodynamic equilibrium models.

Figure 13.2 Thermodynamic Equilibrium Model of Swiss Bottom Ash

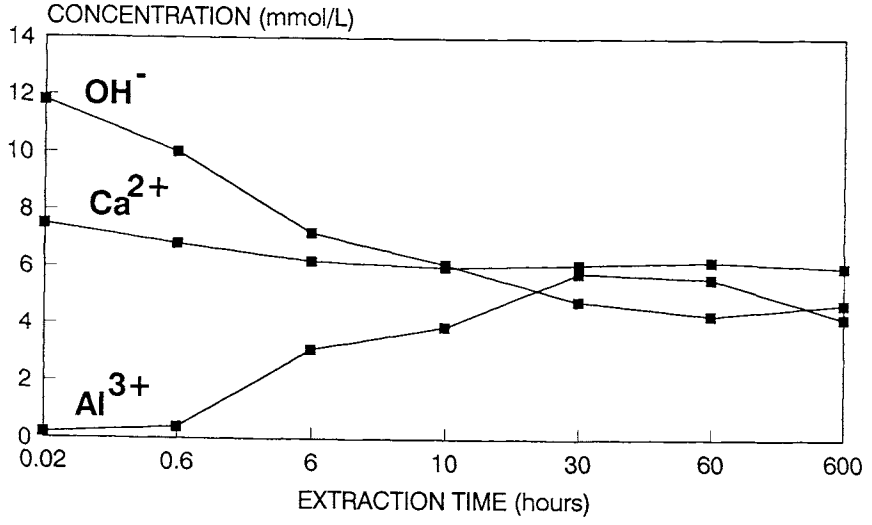

After Stämpfli et al., 1990

Conversely, Figure 13.3 depicts a heterogeneous reaction where the change in molybdenum concentration in the aqueous phase in the presence of MSW bottom ash does not reach equilibrium over the time course of the experiment. The reactions were conducted in a closed system under batch-stirred conditions (Comans et al., 1993). By 200 hours, the aqueous phase concentration of molybdenum has clearly not reached a constant value. If the leaching tests or experiments were designed to evaluate the equilibrium relations of molybdenum with a bottom ash solid phase, and the time frame was less than 200 hours, then no confidence exists to state that equilibrium was achieved because the system is governed by relatively slow kinetics. It could, however, be modelled using a kinetic model.

Figure 13.3 Kinetic Model of Molybdenum Dissolution from MSW Bottom Ash

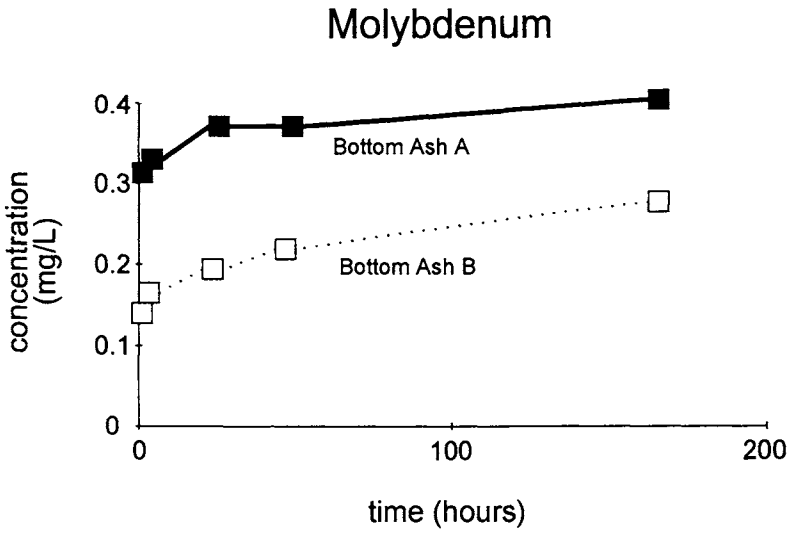

After Comans et al., 1993

As explained previously, the ash system is made complex by the fact that the solid phase is multicomponent, containing many discrete phases each with different solubilities. Like coal ash systems (Dudas, 1981; de Groot et al., 1987), the MSW combustion residue leaching system is dictated by the initial release of readily soluble discrete inorganic salts (e.g. $CaCl_2$, NaCl, KCl) admixed with much more complex glassy aluminosilicate solid phases that leach very slowly.

The most widely used method for obtaining chemical speciation information is the thermodynamic-equilibrium approach (Pankow, 1991). With this method, it is assumed that the leaching system is at equilibrium; the system experiences no changes with time in chemistry, temperature or pressure, and moreover has no tendency to change. The

equilibrium state is controlled by the thermodynamic energy levels of all the chemical constituents involved, including all gases, dissolved species and residue solid phases.

When modelling an actual leaching system, there are likely to be numerous chemical reactions. At system equilibrium, all of the corresponding equilibrium expressions and the various mass balance conditions governing that situation must be satisfied simultaneously. Such systems are usually complicated by the fact that many of the reactions involve species that are also participants in other simultaneously occurring reactions. In recent years, sophisticated computer codes that compute equilibrium speciation even for very complicated situations have been developed. These models will be described in Chapter 15.

As discussed earlier, kinetic models are occasionally needed to represent natural water systems, but they are often difficult to apply. Their application requires a knowledge of specific initial conditions as well as all of the pertinent kinetic rate constants (Pankow and Morgan, 1981a, 1981b). There are some major problems with applying kinetic models to leaching (Pankow, 1991). Although the differential equations used for kinetic reactions can be solved using numerical integration techniques, most leaching systems involve complex coupled equations. In addition, rate constants are typically not known as well as equilibrium constants, and complex kinetic laws are often observed (Pankow, 1991).

13.1.2 Ionic Strength, Ion Activity, Activity Coefficients

Many leaching solutions contain high concentrations of dissolved solids or ionic solutes. The presence of these solutes imparts an ionic strength to the leaching solution. Frequently, MSW incinerator residue leachates have ionic strengths (I) that exceed those found in seawaters and brines. At moderate to high ionic strengths, the leaching system departs from ideal behaviour since reactants can be blocked from colliding with each other, thus diminishing their apparent concentration in solution. Reactants can also be pushed closer together, facilitating collisions and increasing apparent concentrations. This departure from ideal behaviour should be understood because it influences the type of equilibrium constants we use to describe leaching and model leaching.

Ionic strength, (I), is determined by

$$I = \frac{1}{2} \sum m_i z_i^2 \qquad (13.1)$$

where

I = ionic strength in units of moles/litre,
m_i = the concentration in moles/litre of the ith ion
z_i = the charge of the ith ion (dimensionless).

Ionic strengths for leachates can range from 0.05M (high L/S tests of bottom ash) to 20M (low L/S leaching tests of ESP ash).

The presence of concentrations of ions in a leaching solution can impact the thermodynamics of reactions. Typically, leaching solutions have sufficient ionic strength that the solution must be classified as non-ideal. Under such conditions, the concentration of solute, [i], must be corrected to describe the solute's activity. At low ionic strengths, the activity of the solute may decrease if other dissolved counter ions in solution shield the ion from participating in chemical reactions. Conversely, at high ionic strength, the activity of the solute may increase if the solute is "salted out" or pushed into closer association with a potential reactant than what would occur under dilute conditions.

The activity of species i is represented as {i} and is defined as

$$\{i\} = \gamma_i[i] \tag{13.2}$$

where

γ_i is the unitless single ion activity coefficient
[i] is the concentration of solute i.

Usually, γ values are less than 1.0, depicting that a solute's activity has an effective concentration that is less than the actual concentration in solution. Under ideal conditions in very dilute systems, γ values are 1.0 and {i} = [i].

There are a number of ways to calculate γ values for ions in solution (Pankow, 1991; Pytkowicz, 1983). As shown in Table 13.2, at least five methods exist.

They are very much dependent on the ionic strength range of the leaching solution. The first four are based on the electrostatic approach developed by Debye and Hückel; they are appropriate for more dilute solutions. The fifth is based on the work of Pitzer and coworkers (ie. Pitzer, 1979, 1981) who substantially modified the Debye-Hückel approach; it is appropriate for more concentrated solutions.

The Pitzer equation contains a first, second, and third virial expansion term beyond the Debye-Hückel term. The expansion terms account for complex ion interactions that occur with increasing ionic strength. A term for neutral species interactions (λ) has been added by Harvie et al. (1984). Equations are also presented by Harvie et al. (1984) for γ_X and γ_N; single ion activity coefficients for anion X and neutral species N, respectively. In the Pitzer equation, m_c and z_c are the molality and charge of cation C. N_c is the total number of cations in solution. Additional terms include:

Table 13.2
Methods for Determining Activity Coefficients

Name	Equation	Applicable Ionic Strength Range
Debye-Hückel[a]	$\log \gamma_i = -Az_i^2\sqrt{I}$	$I < 10^{-2.3}$
Extended Debye-Hückel[a]	$\log \gamma_i = -Az_i^2[\sqrt{I}/(1 + B\alpha\sqrt{I})]$ α is a size parameter for ion i; it should not be confused with the activity	$I < 10^{-1.0}$
Güntleberg[a]	$\log \gamma_i = -Az_i^2[\sqrt{I}/(1 + \sqrt{I})]$ equivalent to Extended form with an average value of $\alpha = 3$	$I < 10^{-1.0}$
Davies[a]	$\log \gamma_i = -Az_i^2[(\sqrt{I}/(1 + \sqrt{I})) - 0.2I]$	$I < 0.5$
Pitzer[b]		$I < 20M$

$$\ln\gamma_M = z_M^2 F + \sum_{a=1}^{N_a} m_a(2B_{Ma} + ZC_{Ma}) + \sum_{c=1}^{N_c} m_c(2\Phi_{Mc} + \sum_{a=1}^{N_a} m_a\psi_{Mca}) + \sum_{a=1}^{N_a-1}\sum_{a'=a+1}^{N_a} m_a m_{a'}\psi_{aa'M} + |z_M|\sum_{c=1}^{N_c}\sum_{a=1}^{N_a} m_c m_a C_{ca} + \sum_{n=1}^{N_n} m_n(2\lambda_{nM})$$

[a] Equations for activity coefficient γ_i where the activity $\alpha_i = \gamma_i m_i$. For the ionic strength ranges applicable for the equations, $\zeta_i \sim \gamma_i \sim y_i$ where ζ_i and y_i are the activity coefficients on the mole fraction and molarity concentration/activity scales, respectively. The parameter A depends on T(K) according to the equation $A = 1.82 \times 10^6(\epsilon T)^{-3/2}$ where ϵ is the temperature-dependent dielectric constant of water. $B = 50.3(\epsilon T)^{-1/2}$. For water at 298 K (25°C), A = 0.51 and B = 0.33.

[b] The form of the Pitzer equation is for the single ion activity coefficient for a cation M (Harvie et al., 1984).

$$F = -A^{\Phi}\left(\frac{\sqrt{I}}{1+1.2\sqrt{I}} + \frac{2}{1.2}\ln(1+1.2\sqrt{I})\right)$$

$$+ \sum_{c=1}^{N_c}\sum_{a=1}^{N_a} m_c m_a B'_{ca}$$

$$+ \sum_{c=1}^{N_c-1}\sum_{c'=c+1}^{N_c} m_c m_{a'} \Phi_{cc'}$$

$$+ \sum_{a=1}^{N_a-1}\sum_{a'=a+}^{N_a} m_a m_{a'} \Phi_{aa'}$$

where the 1.2 value is a universal empirical value.

$$C_{MX} = C^{\phi}_{MX}/2|z_M z_X|^{1/2},$$

$$Z = \sum_i |z_i| m_i, \text{ and}$$

$$A^{\Phi} = 1/3(2\pi N_o d_w|1000)^{1/2}(\varepsilon^2/DkT)^{3/2}$$

where N_o is Avagadro's Number, d_w is the density of water, ϵ is static dielectric constant of water at temperature T, k is the Boltzmann's constant, and e is electronic charge. A^{Φ} is 0.392 for water at 25°C.

The second virial coefficients B are defined as:

$$B_{MX} = \beta^{(0)}_{MX} + \beta^{(1)}_{MX} g(\alpha_{MX}\sqrt{I}) + \beta^{(2)}_{MX} g(12\sqrt{I})$$

$$B'_{MX} = \beta^{(1)}_{MX} g'(\alpha_{MX}\sqrt{I})/I + \beta^{(2)}_{MX} g'(12\sqrt{I})/I$$

where the functions g and g' are:

$$g'(\chi) = -2(1-(1+\chi+\frac{\chi^2}{2})e^{-\chi})/\chi^2$$

$$g(\chi) = 2(1-(1+\chi)e^{-\chi})/\chi^2$$

where $\chi = \alpha_{MX}\sqrt{I}$ which simplifies to $12\sqrt{I}$. Further, if M or X is univalent, $\alpha_{MX} = 2.0$. For 2-2 or higher valence pairs, $\alpha_{MX} = 1.4$. Simplified versions of the Pitzer equations

can be found in Whitfield (1975a,b) and Millero & Schreiber (1982). Pytkowicz (1983) reviews many ion association, ion interaction and activity determination methodologies.

The Davies Equation is probably the most appropriate for use with dilute leaching solutions. It is semi-empirical with an applicable range that covers the values of I most often seen in like bottom ash leachates ash leaching solutions. Table 13.3 provides some values of γ_i for solutes of valency 1 through 5 for ionic strengths appropriate to ash leaching systems.

Table 13.3
Values of γ_i for Solutes of Valency 1-5, Based on the Davies Equations

Ionic Strength (I)	Valency, z_i				
	1	2	3	4	5
			γ_i		
0.001	0.965	0.867	0.726	0.566	0.411
0.002	0.952	0.820	0.641	0.453	0.290
0.005	0.927	0.739	0.506	0.298	0.151
0.010	0.902	0.662	0.396	0.192	0.076
0.025	0.860	0.546	0.256	0.089	0.023
0.030	0.850	0.522	0.232	0.074	0.017
0.050	0.822	0.455	0.170	0.043	0.007
0.100	0.782	0.373	0.109	0.019	0.002

Data compiles from Lindsay, 1979.

Under conditions of higher ionic strength, the calculation of single ion activity coefficients is more complicated (Pytkowicz, 1983). Leachates from ESP ash or scrubber residues have ionic strengths ranging from 0.5 to 20 M. These solutions are more akin to seawater and brines in that (i) ionic strengths are very high, (ii) the solutions are complex and contain many electrolytes, and (iii) complex interactions like ion pair formation (i.e. $Ca^{2+} + Cl^- \rightleftharpoons CaCl^+$) can have a significant impact on reducing both overall ionic strength and the activity of the individual paired ions.

Two approaches have been developed to calculate activities in complex electrolyte solutions (Stumm and Morgan, 1981; Drever, 1988). The first involves the concept of ion association, particularly the formation of ion pairs. Usually, ion activities are experimentally determined in various simple electrolyte solutions. This is obviously difficult to compare to complex electrolyte solutions like seawater or brines with many dissolved species. Consequently, a second approach involving specific ion interactions was developed. The extended Debye-Hückel approach was made applicable for higher

ionic strengths by adding additional interaction terms or virial coefficients to account for short range interactions between oppositely charged ions (Guggenheim, 1966). Guggenheim's modifications were further changed by Pitzer & Brewer (1961), Scatchard (1968) and Pitzer (1973), who all refined the second virial coefficient. This equation was found to be valid up to an ionic strength of about 4M. Whitfield (1975a,b) modified Pitzer's equations to calculate single ion activity coefficients. Values for seawater-like solutions (up to 3.0 M) were calculated. These values are shown in Table 13.4 and are useful approximations for APC residue leachates.

Table 13.4
Values for γ_i for Various Solutes in Brines

Ion/Ionic Strength	0.2	0.4	0.6	0.7	0.8	1	2	3
H^+	0.744	0.716	0.71	0.711	0.714	0.724	0.826	0.995
Na^+	0.724	0.677	0.652	0.643	0.637	0.626	0.614	0.634
K^+	0.709	0.653	0.62	0.607	0.597	0.581	0.537	0.528
NH_4^+	0.707	0.649	0.615	0.603	0.592	0.575	0.531	0.517
Be^{2+}	0.206	0.128	0.092	0.081	0.071	0.058	0.029	0.019
Mg^{2+}	0.299	0.248	0.228	0.222	0.219	0.214	0.238	0.306
Ca^{2+}	0.284	0.23	0.206	0.199	0.194	0.188	0.19	0.224
Sr^{2+}	0.284	0.229	0.205	0.197	0.191	0.183	0.178	0.201
Ba^{2+}	0.273	0.215	0.188	0.179	0.172	0.162	0.144	0.148
Zn^{2+}	0.288	0.229	0.201	0.192	0.184	0.173	0.142	0.125
Cu^{2+}	0.273	0.215	0.188	0.18	0.173	0.164	0.149	0.156
Pb^{2+}	0.193	0.119	0.086	0.075	0.066	0.054	0.026	0.017
Fe^{2+}	0.281	0.227	0.204	0.197	0.192	0.186	0.189	0.225
Co^{2+}	0.289	0.234	0.211	0.205	0.2	0.194	0.204	0.248
Ni^{2+}	0.29	0.237	0.215	0.208	0.204	0.198	0.21	0.259
Mn^{2+}	0.3	0.243	0.218	0.21	0.205	0.197	0.197	0.225
UO_2^{2+}	0.312	0.261	0.242	0.237	0.234	0.233	0.267	0.345
F^-	0.694	0.628	0.587	0.571	0.558	0.535	0.468	0.435
Cl^-	0.744	0.71	0.695	0.691	0.689	0.687	0.712	0.778
Br^-	0.753	0.726	0.718	0.717	0.718	0.723	0.786	0.892
I^-	0.768	0.751	0.753	0.757	0.762	0.777	0.889	1.059
OH^-	0.711	0.658	0.628	0.618	0.609	0.597	0.578	0.596
$H_2PO_4^-$	0.662	0.577	0.523	0.502	0.483	0.451	0.353	0.299
NO_2^-	0.69	0.624	0.585	0.571	0.559	0.539	0.488	0.469
NO_3^-	0.718	0.665	0.634	0.622	0.612	0.596	0.551	0.533
SO_4^{2-}	0.235	0.169	0.136	0.125	0.116	0.101	0.064	0.05
HPO_4^{2-}	0.245	0.167	0.128	0.115	0.104	0.087	0.046	0.031
CO_3^{2-}	0.237	0.162	0.127	0.1125	0.105	0.091	0.057	0.043
PO_4^{3-}	0.05	0.024	0.015	0.012	0.01	0.008	0.003	0.001

Based on the Pitzer Equations (from Whitfield (1975a,b) with kind permission from Elsevier Sciences Ltd., The Boulevard, Langford Lane, Kidlington OX5 1GB, UK)

Subsequent modifications (Pitzer & Mayorga, 1973; Pitzer & Kim, 1974) ultimately resulted in the addition of more interaction terms or virial coefficients to account for more complex ion interactions between ions of like charge and ions and water that occur at even higher ionic strength (up to 20 M) and thus define the Pitzer equations. The Pitzer equations have been modified by Harvie & Weare (1980) and Harvie et al. (1984) for complex electrolyte solutions like seawater. Interaction terms (β^o, β^1, C^ϕ, λ) between ions are found in Pitzer & Mayorga (1973), Pitzer and Kim (1974), Pitzer, (1979), Harvie & Weare (1980), Harvie et al. (1984) and Kim & Frederick (1988). The model has been validated for many solutes under very high ionic strengths. Pitzer equations have been added to some geochemical thermodynamic equilibrium models (i.e. SOLMINEQ 88, PHREQPITZ, SOLTEQ) for use in modelling brine or cement geochemistry.

Activity coefficients for aqueous neutral species can be determined using the following relationship (Helgeson, 1969):

$$\log\gamma_i = \alpha_1 I \tag{13.3}$$

Typically α_1 is set at 0.1 (Felmy et al. 1984).

The activity coefficients like those shown in Tables 13.3 and 13.4 are useful in understanding departures from ideal behaviour, in evaluating results from modelling efforts using geochemical thermodynamic models and in selection of appropriate equilibrium constants (see section 13.1.4).

13.1.3 Cation/Anion Balances

It is important to introduce the concept of cation and anion balances in leaching solutions. The sum of all positively charged ions (cations) must equal the sum of all negatively charged ions (anions). Leaching solutions can be evaluated for this balance; it provides information on the adequacy of an analytical protocol in quantifying all dissolved constituents in solution. This concept is also employed in modelling efforts described in Chapter 15.

In aqueous systems, bulk solutions do not carry any charge. They are electroneutral. A modified electoneutrality equation can be used to depict this fundamental requirement.

$$\sum_i z_i c_{i_{(\text{positive ions})}} = \sum_i z_i c_{i_{(\text{negative ions})}} \tag{13.4}$$

where

z_i = the charge on ion i in positive or negative integer values (unitless),
c_i = the concentration of ion i in moles/litre.

The equation can be modified to employ equivalent solutions instead of molar solutions. Equation 13.4 becomes very valuable in assessing the quantitative success in accounting for all dissolved constituents in a leaching solution.

Belevi and Bacchini (1989) have calculated cation and anion balances for bottom ash leachates (Figure 13.4) after a 50-hour extraction. Generally close agreement between the sums of cations and anions was seen. A more detailed calculation of cation-anion balances is provided by Stämpfli et al. (1990) for a wet bottom ash from a Swiss incinerator. Balances were conducted periodically over the 415-hour time course for the leaching of the bottom ash into a closed system (Table 13.5). As shown in the table, the largest discrepancy between cations and anions (1.7 meq/litre) accounts for only about 7% of the total amount of cations and anions in the system (up to 25.7 meq/litre).

Table 13.5
Cation-Anion Balances Over Time

		Extraction Time					
Parameter		30 min	5 h	9 h	24 h	48 h	415 h
Ca^{2+}	[meq/l]	10.1	9.3	9.3	9.8	10	9.4
$[Ca(OH)]^{+}$	[meq/l]	1.2	0.7	0.7	0.5	0.5	0.5
Na^{+}	[meq/l]	2.1	2.3	2.3	2.5	2.5	2.8
K^{+}	[meq/l]	0.5	0.6	0.8	0.7	0.7	0.7
Cations	[meq/l]	13.9	13	13.1	14	14	13.4
$[Al(OH)_4]^{-}$	[meq/l]	0.5	2.9	3.6	5.2	5	4
OH^{-}	[meq/l]	9.6	6.3	5.6	4.3	4	4.4
Cl^{-}	[meq/l]	2.2	2.5	2.6	2.9	2.8	3.1
$[SO_4]^{2-}$	[meq/l]	0.3	0.2	0.2	0.2	0.2	0.2
Anions	[meq/l]	12.6	12	12	13	12	11.7
Cations-Anions	[meq/l]	1.3	1.1	1.1	0.9	1.7	1.7

After Stämpfli et al., 1990

Thus, the use of such balancing techniques can tell if the analytical scheme is accounting for all of the dissolved constituents of interest. It can also provide information as to the dominancy of the major cations and anions in solution. This can be coupled with mass balances on solids when a residue is leached, i.e. the total dissolved solids that are produced should equal the mass change in the residue when leached in a closed system.

Figure 13.4 Cation-Anion Balance

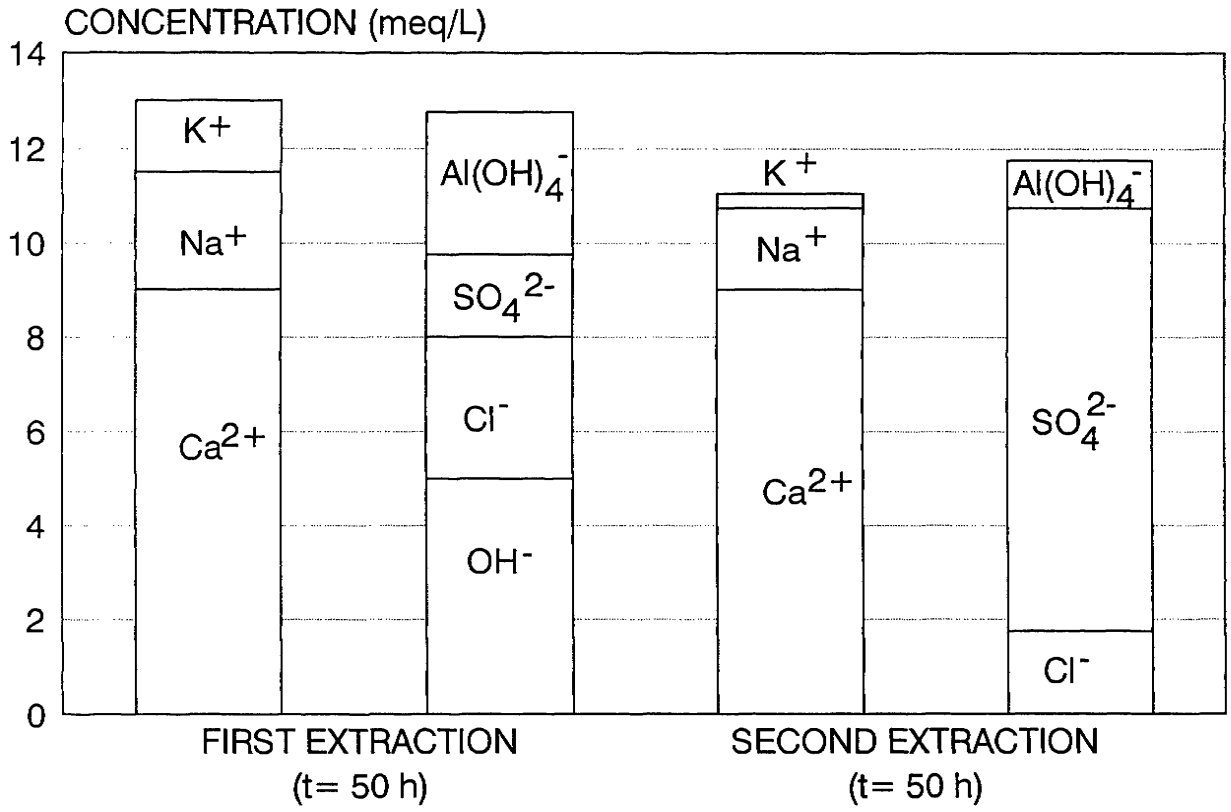

After Belevi and Bacchini, 1989

13.1.4 A Note on General Equilibrium Constants

It is necessary to understand the various methods for determining equilibrium constants as well as the nature of equilibrium constants in order to properly evaluate leaching behaviour, interpret data from field leaching scenarios or leaching tests and model leaching phenomena. The equilibrium constants in the literature or in thermodynamic models are routinely modified or updated during evaluation or modelling.

Consider the following hypothetical dissociation reaction conducted at 25°C (298.15°K) at 1 atmosphere under infinitely dilute conditions:

$$\{HA\} \rightleftharpoons \{H^+\} + \{A^-\} \quad \text{or} \tag{13.5}$$

$$[HA]\gamma_{HA} \rightleftharpoons [H^+]\gamma_{H}^{+} + [A^-]\gamma_{A}^{-} \tag{13.6}$$

Under ideal infinitely dilute conditions, activity coefficients approach unity and activity and concentration become equivalent. The activity equilibrium constant of 25°C under dilute conditions, designated as K, is defined as:

$$K = \frac{\{H^+\}\{A^-\}}{\{HA\}} \text{ or } \frac{[H^+]\gamma_{H^+}[A^-]\gamma_{A^-}}{[HA]\gamma_{HA}} \tag{13.7}$$

Sometimes the equilibrium constant K can be determined experimentally by measuring reactants and products at equilibrium (Rosotti, 1981) under infinitely dilute conditions at 25°C.

More often, K is determined from the Gibbs free energy of formation ($\Delta G_f°$), the standard free energy change of a reaction ($\Delta G_r°$), the standard enthalpy of a reaction ($\Delta H_r°$), and the standard entropy of a reaction ($\Delta S_r°$).

The standard free energy change accompanying a reaction ($\Delta G_r°$) is the sum of free energies of formation ($\Delta G_f°$) of the products in their standard state minus the free energies of formation of the reactants in their standard state:

$$\Delta G_r° = \sum \Delta G_f° \text{ products} - \sum \Delta G_f° \text{ reactants} \tag{13.8}$$

$\Delta G_r°$ can be related to K by the following:

$$\Delta G_r° = RT\ln K \tag{13.9}$$

At 25°, R = 0.08314 KJ/mole K and T = 298.15 °K such that

$$\Delta G_r° = -1.364 \log K \quad \text{or} \tag{13.10}$$

$$\log K = - \frac{\Delta G_r^\circ}{1.364} \qquad (13.11)$$

Therefore, for any reaction, published values for ΔG_f° for the reactants and products can be used to calculate ΔG_r° and therefore K.

Occasionally, ΔG_r° can be calculated from changes in the standard enthalpies of reaction (ΔH_r°) and changes in entropies of reaction (ΔS_r°) using the following:

$$\Delta G_r^\circ = \Delta H_r^\circ - T\Delta S_r^\circ \text{ , where} \qquad (13.12)$$

$$\Delta H_r^\circ = \sum \Delta H_f^\circ \text{ products} - \sum \Delta H_f^\circ \text{ reactants and} \qquad (13.13)$$

$$\Delta S_r^\circ = \sum S^\circ_{\text{products}} - \sum S^\circ_{\text{reactants}} \qquad (13.14)$$

Calorimetric measurements of the heat of solution are used to calculate the heat of formation (ΔH_f°). Calorimetric measurements of heat capacity are used to calculate entropy (ΔS°). If these are known for the reactants and products, then ΔG_r° and K can be calculated.

Thermodynamic data bases containing various ΔG_f°, ΔH_f° and ΔS° values for reaction constituents are found in the National Institute of Standards and Technology (formerly the National Bureau of Standards) Technical Note series 270 (Parker et al., 1971; Schumm et al., 1973; Wagman et al., 1968; 1969; 1971; 1981) and in Wagman et al. (1982). They are also found in a U.S. Geological Survey compilation (Robie et al., 1978, 1979;) and other compilations (Baes and Mesmer, 1976; Smith and Martell, 1976; Naumov et al., 1974; Lindsay, 1979). These databases, particularly Wagman et al. (1982), are deemed to be the most complete, annotated and accurate (Allison et al., 1990; Felmy et al., 1984; Krupka et al., 1988). They also form the basis for the geochemical source codes in the models presented in Chapter 15.

Usually, three types of equilibrium constants are used in aqueous geochemistry applications. They are:

K	an activity constant at infinite dilution, used most frequently because of its basis on ΔG_f°,
K^c	a concentration constant, where all reactants are expressed in terms of analytical concentration at some specified ionic strength I, and
K^m (or K')	a mixed constant, where all terms are given in concentration except H^+, OH^- and e^-, which are given as activities.

Using equations (13.5) through (13.7) as examples, the three equilibrium values can be interrelated:

$$K = \frac{\{H^+\}\{A^-\}}{\{HA\}} = \frac{[H^+]\gamma_{H^+}[A^-]\gamma_{A^-}}{[HA]\gamma_{HA}} = \frac{K^c\gamma_{H^+}\gamma_{A^-}}{\gamma_{HA}} = \frac{K^m\gamma_{A^-}}{\gamma_{HA}} \quad (13.15)$$

As indicated above, the thermodynamic databases mentioned above usually present K. Frequently, the literature contains K^c or K^m values; the geochemical models also convert K to K^m when H^+, OH^- or e^- are directly inputted as fixed species in the model.

Equilibrium constants are temperature dependent. Most are reported at 25°C. To correct them for other temperatures, the Van't Hoff relationship is used:

$$\log K_T = \log K_{T_r} - \frac{\Delta H_r^\circ}{2.3R}\left(\frac{1}{T} - \frac{1}{T_r}\right) \quad (13.16)$$

where

K_T = the constant at a specified temperature,
K_{T_r} = the reference constant at 298.15 K (25°C),
ΔH_r° = the enthalpy of reaction,
T = the specified temperature (K),
T_r = the reference temperature (K),
R = the ideal gas constant.

13.2 SOLUTION COMPLEXATION AND SPECIATION

It is important to understand the role that complexation plays in controlling the speciation of dissolved elements in solution. The solution phase speciation of an element can impact its mobility in the environment, its bioavailability, and its ability to participate in precipitation or sorption reactions. Soluble complexation is also an important feature of modelling efforts presented in Chapter 15.

In almost all leaching solutions, the solutes of interest (e.g. trace metal species such as Pb^{2+}) are present as soluble complexes with various ligands (e.g. Cl^-, OH^-, organic matter) such that the concentration of the uncomplexed or "free" solute (e.g. Pb^{2+}) is small compared to various complexes (e.g. $PbCl^-$, $PbCl_2^\circ$, $Pb(OH)^-$, $Pb(OH)_2^\circ$, $Pb(OH)_3^+$). This has ramifications in the interpretation of the leaching system and the mechanisms that occur in the system.

In pure solution, most dissolved metal atoms are usually surrounded by six waters of hydration or "aquo" complexes. They form a defined geometrical structure around the atom (Drever, 1988). Complexation can be defined as the displacement of these coordinated water molecules by other ligands. Two types of soluble complexes can occur for elements in a solution where ligands exist (Evans, 1989). Outer sphere

complexes, or "ion pairs", can form. These are relatively weak electrostatic interactions between a cationic element (e.g. Pb^{2+}) and an anionic complexing ligand (e.g. Br^-) to form a soluble complex ($PbBr^-$). With weak, outer shell complexes, one or both of the participants retains a hydration structure that solubilises the reactant. Inner sphere complexes are strong associations between an element and a ligand where a covalent bond is formed between the element of interest (e.g. Pb^{2+}) and the ligand (OH^-) to form a soluble, but more tightly bound complex ($Pb(OH)^-$). These complexing ligands can be monodentate (forming one association) or multidentate (forming many associations, termed a chelate). Most ligands are conjugate bases of weak acids. The extent of complexation depends on the relative amounts of the elements and ligands, as well as the pH of the system. In general, complexes between monodentate ligands and metal ions from the first column of the periodic chart are weak. Figure 13.5 depicts some of the various complexes that can form (Stumm and Morgan, 1981).

Figure 13.5 Metal Speciation in Solution

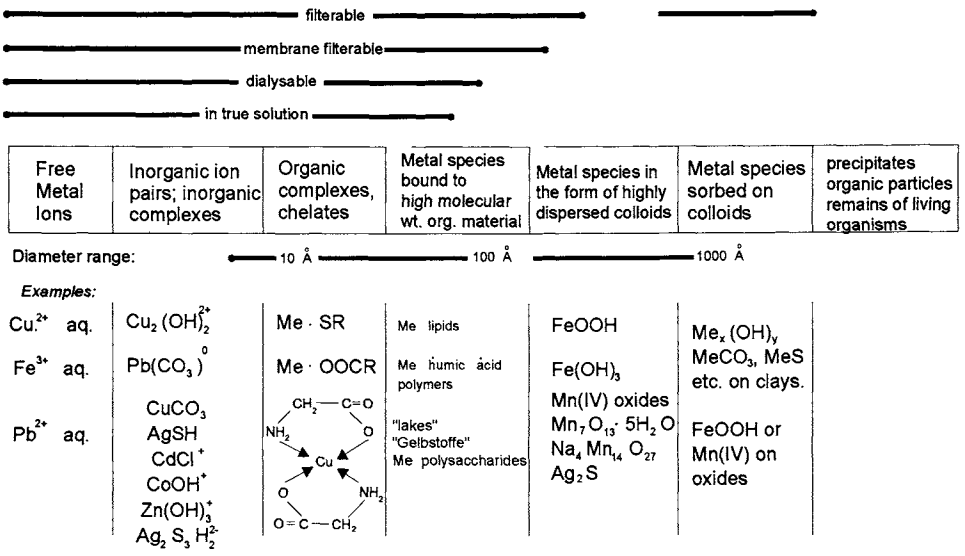

From Stumm and Morgan, 1981. ©1981 by John Wiley & Sons, Inc. Reprinted by permission of John Wiley & Sons, Inc.

When a leaching solution is quantified using ion chromatography, flame or graphite furnace atomic absorption spectrometry, inductively coupled plasma spectrometry or X-ray fluorescence, it tells us the analytical concentration of an element in all of its complexed forms and uncomplexed form in the leaching solution, $C_{T,i}$. It does not

differentiate the uncomplexed from the complexed element. The actual concentration of an element that is in an uncomplexed form is usually much less. Yet it is this uncomplexed fraction of the $C_{T,i}$ that participates in precipitation/dissolution reactions and in many adsorption/desorption reactions in the leaching system.

We can calculate the concentration of a solute i, [i], by:

$$[i] = \frac{C_{T,i}}{a} \tag{13.17}$$

where $C_{T,i}$ is the analytical concentration of the solute i and a is a term derived from the mass balance on an element or solute and various equilibrium relations describing how i is complexed. We can then calculate the activity of i, {i} by using equation (13.2).

13.2.1 Solution Complexation Equilibria

The nomenclature used in depicting solution phase complexation reactions follows the description by Pankow (1991). Consider the formation reaction where metal cation M and ligand anion L combine to form the complex ML:

$$M + L \rightleftharpoons ML \tag{13.18}$$

The stability or formation constant, K, is described by:

$$K = \frac{\{ML\}}{\{M\}\{L\}} \tag{13.19}$$

The reaction shown in Equation 13.18 can be written as a dissociation reaction where ML dissociates to M and L:

$$ML \rightleftharpoons M + L \tag{13.20}$$

The instability or dissociation constant for this reaction is the inverse of the stability constant:

$$1/K = \frac{\{M\}\{L\}}{\{ML\}} \tag{13.21}$$

The strength of the complex that forms is a function of the value of the stability constant. High values ($>10^8$) denote strong complexes. Low values ($<10^2$) denote weak complexes. Table 13.6 depicts the relative strengths of stability constants and dissociation constants.

Table 13.6
Formation and Dissociation Constant Strengths

Type of Constant	Strength of Complex		
	Weak	Moderately Strong	Strong
Metal/Ligand formation (stability) constant	$<10^2$	$\sim 10^5$	$>10^8$
Metal/Ligand dissociation (instability) constant	$>10^{-2}$	$\sim 10^{-5}$	$<10^{-8}$

Reprinted with Permission from Pankow, 1991. Copyright Lewis Publishers, an imprint of CRC Press. Boca Raton, Florida. ©1991

There are other types of stability constants for formation reactions that are summarised in Table 13.7 (Pankow, 1991). Knowledge as to the type of stability constant used in the evaluation of leaching data or in modelling leaching is important if it is to be done correctly.

13.2.2 An Example of Lead Complexation in a Hypothetical Leaching Solution

As an example, a simple solution containing only Pb^{2+}, H_2O, H^+, OH^-, Cl^-, Br^- and SO_4^- is assumed. Ionic strength effects are neglected for simplification. The concentration of ligands is set at 10^{-3}M and $\{H^+\}$ is set at $1x10^{-10}$ (pH = 10). Using the nomenclature in Table 13.7, consider the following complexation reactions that can occur for lead in this very simplified system.

$$Pb^{2+} + H_2O \rightleftharpoons PbOH^+ + H^+ \quad (\log {}^*K = 7.70) \qquad (13.22)$$

$$Pb^{2+} + Cl^- \rightleftharpoons PbCl^+ \quad (\log K_1 = 1.60) \qquad (13.23)$$

$$Pb^{2+} + 2Cl^- \rightleftharpoons PbCl_2^0 \quad (\log K_2 = 1.78) \qquad (13.24)$$

$$Pb^{2+} + Br^- \rightleftharpoons PbBr^+ \quad (\log K_3 = 1.77) \qquad (13.25)$$

$$Pb^{2+} + SO_4^{2-} \rightleftharpoons PbSO_4^o \quad (\log K_4 = 2.62) \qquad (13.26)$$

Table 13.7
Nomenclature for Complexation Constants

When a free, unprotonated ligand combines with a metal ion, a simple K (stability constant) is used with subscript (1,2,3, etc.) to identify the number of ligands:

$$M+L \rightleftharpoons ML \qquad K_1 = \frac{\{ML\}}{\{M\}\{L\}}$$

$$ML + L \rightleftharpoons ML_2 \qquad K_2 = \frac{\{ML_2\}}{\{ML\}\{L\}}$$

$$ML_2 + L \rightleftharpoons ML_3 \qquad K_3 = \frac{\{ML_3\}}{\{ML_2\}\{L\}}$$

When the reactions presented above are added together, a β notation is used to depict additive values of stability constants:

$$M+L \rightleftharpoons ML \qquad \beta_1 = K_1 = \frac{\{ML\}}{\{M\}\{L\}}$$

$$M+2L \rightleftharpoons ML_2 \qquad \beta_2 = K_1K_2 = \frac{\{ML_2\}}{\{M\}\{L\}^2}$$

$$M+3L \rightleftharpoons ML_3 \qquad \beta_3 = K_1K_2K_3 = \frac{\{ML_3\}}{\{M\}\{L\}^3}$$

When the reacting ligand is protonated, an asterisk (*) is used to modify the stability constant, denoting the presence of protons:

$$M + HL \rightleftharpoons ML + H^+ \qquad {}^*K_1 = \frac{\{ML\}\{H^+\}}{\{M\}\{HL\}}$$

$$ML + HL \rightleftharpoons ML_2 + H^+ \qquad {}^*K_2 = \frac{\{ML_2\}\{H^+\}}{\{ML\}\{HL\}}$$

Table 13.7 Continued

$$ML_2 + HL \rightleftharpoons ML_3 + H^+ \qquad {}^*K_3 = \frac{\{ML_3\}\{H^+\}}{\{ML_2\}\{HL\}}$$

If the reactions presented above are additive, then:

$$M + HL \rightleftharpoons ML + H^+ \qquad {}^*\beta_1 = {}^*K_1 = \frac{\{ML\}\{H^+\}}{\{M\}\{HL\}}$$

$$M + 2HL \rightleftharpoons ML_2 + 2H^+ \qquad {}^*\beta_2 = {}^*K_1{}^*K_2 = \frac{\{ML_2\}\{H^+\}^2}{\{M\}\{HL\}^2}$$

$$M + 3HL \rightleftharpoons ML_3 + 3H^+ \qquad {}^*\beta_3 = {}^*K_1{}^*K_2{}^*K_3 = \frac{\{ML_3\}\{H^+\}^3}{\{M\}\{HL\}^3}$$

For the reaction of a metal ion with OH^-, since the hydroxide is not protonated, a simple stability constant with the subscript H denoting hydroxide is used:

$$M + OH^- \rightleftharpoons MOH \qquad K_{H1} = \frac{\{MOH\}}{\{M\}\{OH^-\}}$$

When the reacting ligand is water and since H_2O is the HL version of the OH^- ligand, the following notation is used:

$$M + H_2O \rightleftharpoons MOH + H^+ \qquad {}^*K_{H1} = \frac{\{MOH\}\{H^+\}}{\{M\}}$$

The equations depict a hydrolysis reaction [equation (13.22)], a monodentate and bidentate complexation reaction [equations (13.23) and (13.24)] and two monodentate complexations of various bond strengths [equation (13.25) and (13.26)].

An important consideration in defining solution speciation and the distribution of lead in the solution is as follows: what percentage of the total analytical lead in solution, $C_{T,Pb}$, is the uncomplexed free ion (Pb^{2+}) and what is complexed as $PbOH^+$, $PbCl^+$, $PbCl_2^\circ$, $PbBr^+$ and $PbSO_4^\circ$?

First, the mass balance equation for $C_{T,Pb}$ must be identified:

$$C_{T,Pb} = Pb^{2+} + PbOH^+ + PbCl^+ + PbCl_2^\circ + PbBr^+ + PbSO_4^\circ \qquad (13.27)$$

By combining equations (13.22) through (13.27), equation (13.27) can be solved in terms of the various K values and $\{Pb^{2+}\}$:

$$\begin{aligned} C_{T,Pb} = {} & \{Pb^{2+}\} + {}^*K\{Pb^{2+}\}/\{H^+\} + \\ & K_1\{Pb^{2+}\}\{Cl^-\} + K_2\{Pb^{2+}\}\{Cl^-\}^2 + \\ & K_3\{Pb^{2+}\}\{Br^-\} + K_4\{Pb^{2+}\}\{SO_4^{2-}\} \end{aligned} \qquad (13.28)$$

Dividing through by $\{Pb^{2+}\}$, the equation reduces to:

$$\frac{C_{T,Pb}}{Pb^{2+}\}} = 1 + {}^*K/\{H^+\} + K_1\{Cl^-\} + K_2\{Cl^-\}^2 + K_3\{Br^-\} + K_4\{SO_4^2 \qquad (13.29)$$

Setting $\{Cl^-\}$, $\{SO_4^{2-}\}$ and $\{Br^-\} = 10^{-3}M$ and $\{H^+\} = 10^{-10}$ (e.g. pH = 10), the equation reduces to:

$$\frac{C_{T,Pb}}{\{Pb^{2+}\}} = 1 + 10^{-17.7} + 10^{-1.4} + 10^{-4.22} + 10^{-1.23} + 10^{-0.18} \qquad (13.30)$$

or

$$\{Pb^{2+}\} = 0.5683\ C_{T,Pb} \qquad (13.31)$$

(or 56.8% of $C_{T,Pb}$ is Pb^{2+}). To determine the relative activities of the other species, equation (13.28) and equations (13.22) through (13.26) can be used such that:

Table 13.8
Bottom Ash Outdoor Lysimeter Leachate Aqueous Element Speciation

Element or Parameter	Conc. (mg/L) or Value	Percent Complexed As[c]														
		Me	MeOH	$MeOH_2$	$MeOH_3$	$MeOH_4$	$MeSO_4$	$Me(SO_4)_2$	$MeHCO_3$	$MeCO_3$	MeCl	$MeCl_2$	$MeCl_3$	MeBrCl	$MeBr_2$	$MeBr_3$	Me-Valerate
Al^{3+}	0.020		2.4	22.6	55.7	18.7											
Sb^{5+}	0.063	99.9															
Ba^{2+}	0.10	99.5															
Ca^{2+}	590	73.8					26.0										
Cu^{2+}	0.59	55.4		2.8			19.6		5.3	5.6	2.7						7.9
Fe^{3+}	0.050			97.4	2.2												
Pb^{2+}	0.0053	29.3					28.5	2.0	4.4	9.5	20.8						3.6
Mg^{2+}	6.5	76.3					23.5										
Mn^{+}	0.32	71.9					22.6				5.2						
Hg^{2+}	0.0006											12.6	4.9	61.3	18.8	1.1	
K^{+}	220	96.7					3.3										
Si^{4+}	2.2		--------(Speciated as H_4SiO_4)----														
Na^{+}	740	97.6					2.3										
Sr^{2+}	4.4	100															
Zn^{2+}	0.068	65.4					26.5	2.8	1.6		3.1						
Br^{-}	30																
Cl^{-}	1700																
SO_4^{-2}	1700																
Organic C[a]	300																
Total Alk.[b]	29																
pH	6.41																
L/S	0.08																

[a]TOC; for modelling purposes this was assumed to be valeric acid. [b]mg/L as CaCO3. [c]Metal or metaloid denoted as Me in either free ion form or as a complex. Note that the charge on the complex is not shown

$$\{PbOH^{+}\} = 10^{-17.7}\ 0.5683C_{T,Pb} = 1.13x10^{-18}C_{T,Pb} \quad (13.32)$$

$$\{PbCl^{+}\} = 10^{-1.4}\ 0.5683C_{T,Pb} = 2.20x10^{-2}C_{T,Pb} \quad (13.33)$$

$$\{PbCl_2^{o}\} = 10^{-4.22}\ 0.5683C_{T,Pb} = 3.42x10^{-5}C_{T,Pb} \quad (13.34)$$

$$\{PbBr^{+}\} = 10^{-1.23}\ 0.5683C_{T,Pb} = 5.88x10^{-2}C_{T,Pb} \quad (13.35)$$

$$\{PbSO_4^{o}\} = 10^{-0.18}\ 0.5683C_{T,Pb} = 0.376C_{T,Pb} \quad (13.36)$$

It should be readily apparent that the complexed species with the largest K value ($PbSO_4^{o}$) plays the most significant role in complexing Pb in accordance with the hierarchy shown in Table 13.6.

Given the fact that leaching solutions contain many solutes and that each metal or metalloid is capable of being complexed by 3 to 4 ligands, the tediousness of such calculations and the utility of geochemical models in computer codes is apparent.

13.2.3 Leaching Solution Speciation

Geochemical models such as MINTEQA2 can be used to examine solution phase speciation. The approach has been applied to two leachates: a bottom ash lysimeter leachate at a low L/S value (0.08) and a dry scrubber residue leachate also at a low L/S value (0.2).

Table 13.8 shows the speciation of elements in the bottom ash leachate. For modelling purposes, the organic carbon was assumed to be valeric acid. As can be seen in the table, a number of complexes are present. Metal sulphate, metal bicarbonate and metal chloride complexes are the most predominant. Valerate will complex copper and lead. In some cases, the free ion is not the principal form of the element in solution. The ionic strength (I) of the leachate is 0.09 M.

Table 13.9 shows the speciation of elements in the dry scrubber residue leachate. For modelling purposes, the organic carbon was assumed to be valeric acid. Unlike the bottom ash leachate, the scrubber residue is more alkaline and of much higher ionic strength (28 M). This extremely high value invalidates the use of Davies-based activity coefficients. This leachate is probably one of the strongest that can be produced under column settings. While the use of MINTEQA2 to model this leachate is inappropriate, the results are presented to show how metal chloride complexes are a predominant form of the aqueous species.

Models can also be used to do iterative calculations over a wide range of pH values. Figure 13.6 shows the speciation of lead over a large pH range for a complex system where O_2(aq) is present.

Figure 13.6 Lead Speciation as a Function of pH

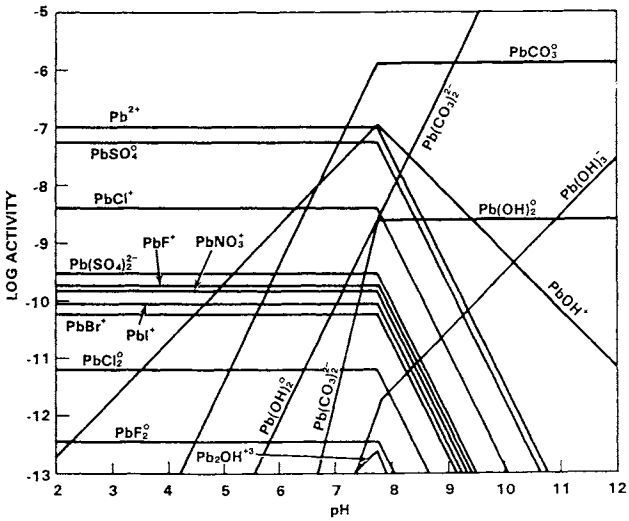

From Rai and Zachara, 1984 Copyright ©1984. Electric Power Research Institute. EPRI (EA-3356) "Chemical Attenuation Rates, Coefficients, and Constants in Leachate Migration". Reprinted with permission

13.3 DISSOLUTION AND PRECIPITATION REACTIONS

Frequently, the mineralogical characteristics of the ash solid phase play the dominant role in controlling all leaching processes. Knowledge as to how the solid phases dissolve or reprecipitate is crucial in evaluating leaching data (Chapter 16), designing or using leaching tests (Chapter 14), relating solid phase speciation data (Chapter 7) to leaching behaviour, and in correctly modelling leaching behaviour (Chapter 15).

The interactions that occur in the ash leaching system (see Figure 12.2, Chapter 12) become more complex when a solid phase is included in the system. The system becomes a heterogeneous one, consisting of a solid phase and a solution phase. Under different conditions, some mineral phases dissolve and secondary mineral phases can form (Warren and Dudas, 1987). Dissolution and precipitation reactions are usually slower than the aqueous phase reactions discussed in Section 13.2. Nevertheless, the more leachable fractions in the ash residues can dissolve relatively quickly and it is relatively safe to adopt the local equilibrium assumption (LEA) as long as the system has approached equilibrium (e.g. on the order of days for many leaching

tests, weeks to months for field leaching scenarios). As discussed under the section in weathering and aging (Section 13.4), some of the solid phases in ash that dissolve very slowly (e.g. aluminosilicates) can only be examined using a kinetic basis and are not able to be evaluated under LEA.

Precipitates that occur in residues can often be amorphous and metastable. Frequently, degrees of oversaturation or undersaturation can exist. Many of the precipitates are co-precipitates that become amorphous semi-solid gels. Pure solid phases do not always form. Isomorphic substitutions, or displacement of atoms in a crystal lattice with atoms of similar size, and the formation of solid solutions (non-crystalline solids) may decrease the activity of the solid phase. The presence of complexing ligands in solution can also increase solubility. Very fine particle sizes are also more soluble than larger crystalline structures. Nonreactive solutes in the solution phase can alter solubilities by their influence in controlling ionic strength.

It is important to introduce some basic concepts describing equilibrium precipitation and dissolution reactions, the equilibrium constants that are used and the nomenclature that is employed. Section 13.3.1 presents that information.

13.3.1 Heterogeneous Dissolution/Precipitation Equilibria

The approach of Pankow (1991) is used to differentiate nomenclature on dissolution/precipitation equilibria. The equilibrium constants for dissolution/ precipitation reactions that produce dissolved ions are usually referred to as K_{sp} values. The subscript "sp" is an abbreviation for "solubility product". The word product refers to the product of ion activities that appears in the expression for the solubility equilibrium constant.

Another type of symbol used for solubility products is the K_{so}. In this symbol, the "s" in the subscript refers again to solubility. The zero, on the other hand, denotes the fact that the constant refers to the specific solubility product for which the identities of the ions in solution are exactly the same as in the solid (Pankow, 1991).

Consider an equilibrium expression describing the precipitation/dissolution of a soluble metal salt (Pankow, 1991):

$$M_mS_s(s) \rightleftharpoons mM^{+s}(aq) + sS^{-m}(aq) \qquad (13.37)$$

At equilibrium, the stoichiometric relationship shown in equation (13.37) becomes:

$$K_{so} = \frac{\{M^{+m}(aq)\}^s\{S^{-s}(aq)\}^m}{\{M_mS_s(s)\}} \qquad (13.38)$$

By convention, the activity of the solid phase is set equal to unity, and the equilibrium expression is simplified to:

Table 13.9
Dry Scrubber Column Leachate Aqueous Element Speciation

Element or Parameter	Concentration (mg/L) or Value	Percent Complexed As[c]							
		Me	MeOH	$MeSO_4$	$MeHCO_3$	$MeCO_3$	$MeCl_2$	$MeCl_3$	Me-Valerate
As	0.21	(speciated as H_2AsO_4 [100%]							
Ca	160,000		93.1	0.2		6.7			
Cd	0.91							100.0	
Cr	2.3	(speciated as $NaCrO_4^-$ [31.4%], $KCrO_4^-$ [68.6%]							
Cu	37.0						2.1	97.9	
Hg	0.003							100.0	
K	22,000	100.0							
Na	7,500	100.0							
Ni	0.10						100.0		
Pb	11,000							100.0	
Zn	550							100.0	
Cl^-	310,000								
SO_4^{2-}	270								
Organic C[a]	45								
Total Alkalinity[b]	540								
pH	9.7								
L/S	0.2								

[a]NVOC; for modelling purposes this was assumed to be valeric acid. [b]meqV/L.
[c]Metal or metalloid denoted as Me in either free ion form or as a complex. Note that the charge on the complex is not shown.

$$K_{sO} = \{M^{+m}(aq)\}^s\{S^{-s}(aq)\}^m \quad (13.39)$$

After conversion to a concentration based system, it becomes:

$${}^cK_{sO} = (M^{+m}(aq))^s(S^{-s}(aq))^m/(\gamma_m)^m(\gamma_S)^s \quad (13.40)$$

where ${}^cK_{sO}$ is the equilibrium constant specific for the reaction and the system it describes. Care must be taken as to which form of the constant is used from the literature. Use of incorrect constants for mechanistic interpretation can lead to gross errors in evaluation of a leaching system.

A large number of sources are available that contain published solubility products. These include Sillen and Martell (1971), Feitknecht and Schindler (1963), Smith and Martell (1976), Robie et al. (1978), Baes and Mesmer (1976), Stumm and Morgan (1981), and Lindsay (1979). The selection of the actual value of a constant should be completed with care in calculations (Stumm and Morgan, 1981). Large differences in values are sometimes observed because (i) a system may be more complex than the simple systems used in determining the various solubility products, (ii) the activity of the solid phases are not always unity and (iii) aqueous phase complexation reactions are overlooked in the determination of published equilibrium constants (Stumm and Morgan, 1981).

13.3.2 Oversaturation/Undersaturation and the Ion Activity Product (IAP)

The identification of the relative degree of potential saturation of solutes in a leaching solution is an important tool in evaluating leaching data and in modelling leaching behaviour. This aspect becomes an important component in the modelling efforts described in Chapter 15. An introduction to the principles is therefore necessary if the tool is to be correctly used.

Returning to equation (13.39), this equilibrium relationship can be used to help determine whether or not a leaching solution is undersaturated (tending towards dissolution) or oversaturated (tending towards precipitation) with respect to a solid phase. Table 13.10 (Pankow, 1991) depicts three conditions applicable to equation (13.39). By convention, the mathematical product of the metal ion activity, $\{M^{+m}(aq)\}^s$, and the salt activity, $\{S^{-s}(aq)\}^m$, is termed the ion activity product (IAP).

The IAP in a slightly modified form is also used in the geochemical models presented in Chapter 15. It is related to the saturation index according to the following (Allison et al., 1990):

$$\text{Saturation Index} = \log \frac{IAP}{K_{sO}} \quad (13.41)$$

Table 13.10
Conditions of Relative Saturation

Condition	State	Implications
$\{M^{+m}(aq)\}^s \{S^{-s}(aq)\}^m < K_{sO}$	Undersaturated	If solid phase is present, some will tend to dissolve; if solid phase is not present, it will not form.
$\{M^{+m}(aq)\}^s \{S^{-s}(aq)\} = K_{sO}$	Saturated	If solid phase is present, no more will dissolve; if solid phase is not present, it will not form.
$\{M^{+m}(aq)\}^s \{S^{-s}(aq)\} > K_{sO}$	Supersaturated	If solid phase is present,more will tend to form; if solid phase is not present, some will tend to form.

As noted by Pankow (1991), if the saturation index is negative, the mineral is undersaturated and will not precipitate out of solution. If the saturation index is positive, the mineral is supersaturated and can precipitate out of solution. If the index is zero, the mineral is present as a solid. The magnitude of the index describes the driving force towards remaining dissolved (a large negative number) or precipitation (a large positive number). The geochemical thermodynamic computer models presented in Chapter 15 utilise this principal in deciding which potential mineral phases will or will not form in a leaching solution. The largest positive indice will precipitate first in response to the driving force.

This principle has been put to use in interpretation of ash leachate. Stämpfli et al. (1990) used this concept to evaluate relative degrees of saturation for bottom ash leachates. Their leachates tended towards undersaturation for certain calcium-containing solid phases.

Fruchter et al. (1990) use the same technique to evaluate the precise nature of the solid phase controlling $\{Ca^{2+}\}$ and $\{SO_4^{2-}\}$ in leachates from coal fly ash. Figure 13.7 depicts a useful graphical tool where the log of the activity of Ca^{2+} is plotted versus the log of the activity of SO_4^{2-}. The equilibrium relationship for two solid phases of interest, $CaSO_4$ (anhydride) and $CaSO_4 \cdot 2H_2O$ (gypsum), are shown as diagonal plots whose y intercepts are the log of the equilibrium K_{sO} for each of the solid phases (or the IAP at equilibrium). Leachate analytical data (e.g. $C_{T,Ca}$, C_{T,SO_4}) were converted to activities (e.g. $\{Ca^{2+}\}$, $\{SO_4^{2-}\}$) using a geochemical thermodynamic equilibrium model (MINTEQA2). The values of $\{Ca^{2+}\}$ were plotted versus the corresponding sample analytical value of $\{SO_4^{2-}\}$. The data fall along the $CaSO_4 \cdot 2H_2O$ boundary, suggesting that some slight under- or oversaturation existed, but that the condition $\{Ca^{2+}\}\{SO_4^{2-}\} = K_{sO(gypsum)}$ was generally met. This becomes an important but simple analytical tool if one desires to identify the nature of the solid phase controlling leaching in the

leaching system. For example, Roy and Griffin (1984) have made extensive use of this approach to understand the nature of the solid phases controlling leaching in various coal fly ash systems as the system ages and weathers over time. From an MSW residue perspective, knowledge of the solid phase controlling solute concentrations in the leachate solution allows for modification or control of the system to either enhance or dissuade leaching.

Figure 13.7 Plot of $\{Ca^{2+}\}$ and $\{SO_4^{2-}\}$ for Coal Ash Leachates

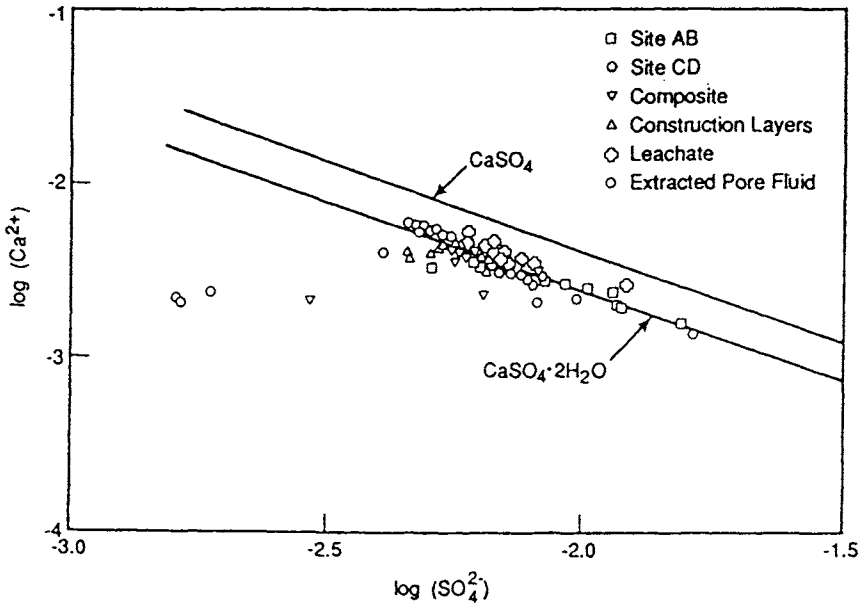

Reprinted with permission from Fruchter et al., 1990. Copyright 1990 American Chemical Society

13.3.3 Metastability

Frequently, solids that precipitate out of solution are still not thermodynamically stable. As the precipitate ages, the solid phase can change its mineralogical structure to become more stable. Such types of transformation, a component of aging reactions, are important in interpreting and modelling field leaching behaviour where solid phases play a strong role in controlling leaching. The concept of metastability of the solid phase, as depicted in Figure 13.8, is introduced by Stumm and Morgan (1981).

Figure 13.8 A Depiction of Metastability

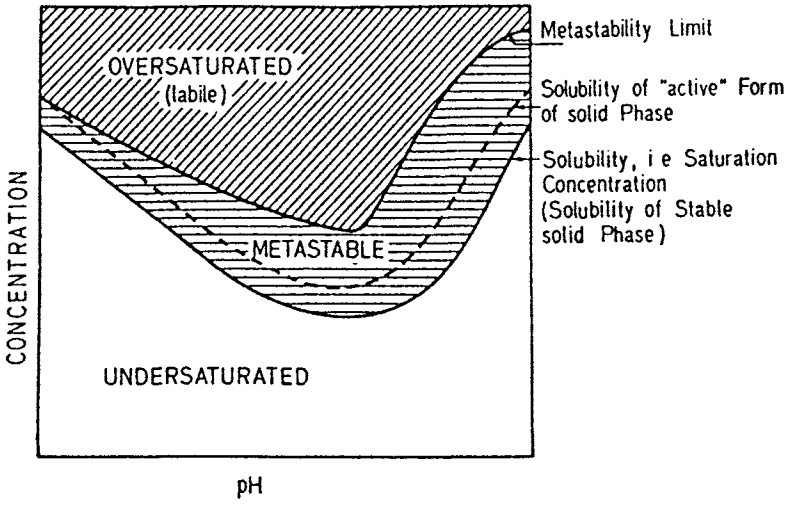

From Stumm and Morgan, 1981. ©1981 by John Wiley & Sons. Reprinted by permission of John Wiley & Sons.

An active form of the solid phase, a very fine precipitate with an unorganised crystalline lattice, is generally formed from oversaturated solutions (Stumm and Morgan, 1981). This active precipitate can exist in metastable equilibrium with the solutes in the solution and may convert or age or ripen only slowly into a more stable inactive form (Stumm and Morgan, 1981). Measurements of the solubility of active forms of the solid phase in question would yield solubility products that are higher than those of the inactive forms. Inactive solid phases whose crystal structure is ordered can also be formed from solutions that are only slightly oversaturated (Stumm and Morgan, 1981).

Hydroxides and sulphides often occur in amorphous and several crystalline forms. Amorphous solids may be active or inactive (Stumm and Morgan, 1981). As noted by Feitknecht and Schindler (1963), initially formed amorphous precipitates or active forms of unstable crystalline forms may transform via two processes during aging. The active form of the unstable form can become inactive or a more stable form can evolve. Deactivation of amorphous compounds may be accompanied by condensation reactions (Stumm and Morgan, 1981). If a metal oxide is more stable than the primarily precipitated hydroxide, dehydration may occur (Stumm and Morgan, 1981). When these reactions occur simultaneously, heterogeneous solids are formed upon aging (Stumm and Morgan, 1981). In dissolution experiments with such nonhomogeneous solids, the more active components are dissolved more readily; that is, the solubility results may depend more upon the quantity of a solid phase present (Stumm and Morgan, 1981).

Precipitates are frequently formed from strongly oversaturated solutions; the conditions of precipitation of the active compound rather than the dissolution of the aged inactive solid are often observed (Stumm and Morgan, 1981). Most solubility products measured for these solids refer to the most active component (Stumm and Morgan, 1981). Heterogeneous equilibria for natural leaching systems contain stable and inactive solids as dominant solid phases. Aging often continues for many years. Solid phases frequently form in nature under conditions of slight supersaturation (Stumm and Morgan, 1981). Thus, use of the correct equilibrium constants should be coupled with speciation methods (Chapter 7) to verify the nature of the solid phases in question.

13.3.4 An Example of Lead Dissolution/Precipitation as $PbSO_4$(s): A Very Simple Leaching System

To illustrate the use of precipitation/dissolution thermodynamics in interpreting and modelling leaching behaviour, it is necessary to start with simple systems to introduce approaches and concepts. This first example makes use of a very simple solid phase solution system. Ionic strength effects will be neglected so that activity, { }, is equal to concentration, ( ). Subsequent examples will add to the complexity of this first example so as to ultimately illustrate the roles of multiple solid phases in equilibrium with each other and with complexing ligands in solution.

$PbSO_4$(anglesite) is frequently found in ash residues. It accounts for some of the available or leachable fraction of lead in combustion residues. Its dissolution is, in part, responsible for the appearance of total dissolved lead ($C_{T,Pb}$) in leaching test or field leachates.

$PbSO_4$(s) exhibits a pH-dependent solubility because the conjugate base, SO_4^{2-} (sulphate), can exhibit pH-dependent protonation reactions that add protons to the base: HSO_4^-(bisulphate) or $H_2SO_4°$(sulphuric acid). Such reactions influence the availability of SO_4^{2-} to precipitate out of solution with Pb^{2+} to form anglesite.

Consider the following equilibrium reaction:

$$\{PbSO_4\} \rightleftharpoons \{Pb^{2+}\} + \{SO_4^{2-}\} \qquad \underline{\log K}: \ -7.79 \qquad (13.42)$$

Equation (13.42) can be rearranged and put in log form such that:

$$\log \{Pb^{2+}\} = -7.79 - \log \{SO_4^{2-}\} \qquad (13.43)$$

It is then necessary to calculate the activity of SO_4^{2-} as a function of pH for substitution into Equation 13.43. H_2SO_4 is a diprotic acid; it exists as the doubly protonated H_2SO_4 (sulphuric acid) at very low pH values (pH <-3), the monoprotonated HSO_4^- (bisulphate)

at low pH values (-3 > pH < 2) and as the unprotonated SO_4^{2-} (sulphate) at moderately low to high pH values (pH > 2). By convention for a diprotic acid (Pankow, 1991) the activity of the SO_4^{2-} when C_{T,SO_4} is fixed at 1 x 10^{-3}M, is calculated as:

$$\{SO_4^{2-}\} = \left(\frac{K_{a,1}K_{a,2}}{\{H^+\}^2 + \{H^+\}K_{a,1} + K_{a,1}K_{a,2}} \right) C_{T,SO_4} \qquad (13.44)$$

where $K_{a,1}$ is the first acid dissociation constant (1 x 10^{-3}) and $K_{a,2}$ is the second acid dissociation constant (1 x 10^{-2}). By selecting various pH values, the SO_4^{2-} concentration as a function of pH can be determined by substitution into equation (13.44):

pH	$\{H^+\}$	$\{SO_4^{2-}\}$
14	1 x 10^{-14}	1 x 10^{-3}
12	1 x 10^{-12}	1 x 10^{-3}
10	1 x 10^{-10}	1 x 10^{-3}
8	1 x 10^{-8}	1 x 10^{-3}
6	1 x 10^{-6}	9.99 x 10^{-4}
4	1 x 10^{-4}	9.90 x 10^{-4}
3	1 x 10^{-3}	9.09 x 10^{-4}
2	1 x 10^{-2}	4.99 x 10^{-4}
1	1 x 10^{-1}	9.09 x 10^{-5}
0	1 x 10^{0}	9.89 x 10^{-6}

If we substitute the log of the $\{SO_4^{2-}\}$ into equation (13.43) and solve for $\{Pb^{2+}\}$ we get:

pH	$P\{Pb^{2+}\}$
14	4.79
12	4.79
10	4.79
8	4.79
6	4.785
4	4.78
3	4.75
2	4.44
1	3.75
0	2.78

The values are plotted as a line in Figure 13.9 in a pC-pH plot. For this simple system, any combination of $\{Pb^{2+}\}$ and pH that is situated above and to the right of the solubility plot (line 1) means that the lead will precipitate out with sulphate to form anglesite. Any combination of $\{Pb^{2+}\}$ and pH that is situated below and to the left of the solubility plot means that lead will stay in solution.

Figure 13.9 $p\{Pb^{2+}\}$ - pH Plot Showing $PbSO_4(s)$ in Equilibrium with $\{Pb^{2+}\}$

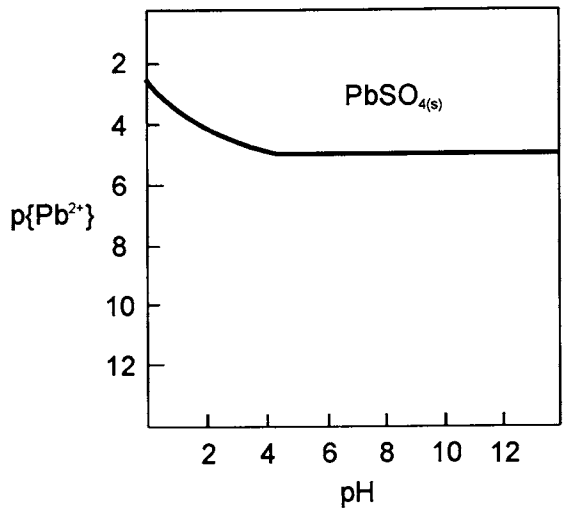

Concentration of SO_4 is $10^{-3}M$

13.3.5 An Example of Lead Dissolution/Precipitation as $Pb(OH)_2(s)$: The Role of Solution Phase Complexation and Amphoterism

The second simple example expands on the one presented in Section 13.3.4. Again, ionic strength effects will be neglected and activity is equal to concentration. A solid phase that exhibits minimum solubility at neutral pH values and maximum solubility at low and high pH (an amphoteric solid) is in equilibrium with a solution which has ligands consisting of hydroxyl anions (OH^-). This example accurately portrays leaching data for a number of metals in ash (see Chapter 16). These ligands form soluble complexes which keep the metal in solution at low and high pH values.

A very simple solid phase-leaching solution system consisting of the solid phase $Pb(OH)_2(s)$ in equilibrium with Pb^{2+} as well as the various solution phase hydrolysis complexes of lead, $Pb(OH)^+$, $Pb(OH_2)°$, $Pb(OH)_3^-$ and $Pb(OH)_4^{2-}$ will be examined.

Consider the following family of equilibrium reactions:

	log K	
$\{Pb^{2+}\} + \{H_2O\} \rightleftharpoons \{Pb(OH)^{+}\} + \{H^{+}\}$	-7.70	(13.45)
$\{Pb^{2+}\} + 2\{H_2O\} \rightleftharpoons \{Pb(OH)_2^{o}\} + 2\{H^{+}\}$	-17.75	(13.46)
$\{Pb^{2+}\} + 3\{H_2O\} \rightleftharpoons \{Pb(OH)_3^{-}\} + 3\{H^{+}\}$	-28.09	(13.47)
$\{Pb^{2+}\} + 4\{H_2O\} \rightleftharpoons \{Pb(OH)_4^{2-}\} + 4\{H^{+}\}$	-39.49	(13.48)
$\{Pb(OH)_2(s)\} + 2\{H^{+}\} \rightleftharpoons \{Pb^{2+}\} + 2\{H_2O\}$	8.16	(13.49)

Looking at the individual hydrolysis species in equilibrium with the solid phase, the result for the first reaction is

	log K	
$\{Pb^{2+}\} + \{H_2O\} \rightleftharpoons \{Pb(OH)^{+}\} + \{H^{+}\}$	-7.70	(13.50)
$+ \{Pb(OH)_{2(s)}\} + 2\{H^{+}\} \rightleftharpoons \{Pb^{2+}\} + 2\{H_2O\}$	8.16	(13.51)
$\{Pb(OH)_{2(s)}\} + \{H^{+}\} \rightleftharpoons \{Pb(OH)^{+}\} + \{H_2O\}$	0.64	(13.52)

Rearranging equation (13.52) results in:

$$\log\{Pb(OH)^{+}\} = 0.46 - pH \quad (13.53)$$

This is plotted as line 1 on Figure 13.10. Like the last example, any combination of $\{Pb^{2+}\}$ and pH above and to the right of the line means that lead precipitates out as $Pb(OH)_2(s)$. Conversely, $Pb(OH)^{+}$ is situated below and to the left of the line. Taking the other possible hydrolysis species and completing the same analysis produces the following sets of relationships:

$$\log\{Pb(OH)_2^{o}\} = -9.59 \quad (13.54)$$

$$\log\{Pb(OH)_3^{-}\} = -19.93 + pH \quad (13.55)$$

$$\log\{Pb(OH)_4^{-}\} = -31.33 + 2pH \quad (13.56)$$

These are plotted as lines 2 to 4 respectively in Figure 13.10.

Figure 13.10 p{Pb^{2+}} - pH Plot Showing $Pb(OH)_2$ in Equilibrium with {Pb^{2+}}, {$PbOH_2^0$}, {$Pb(OH)_3^-$}, {$Pb(OH)_4^{2-}$}

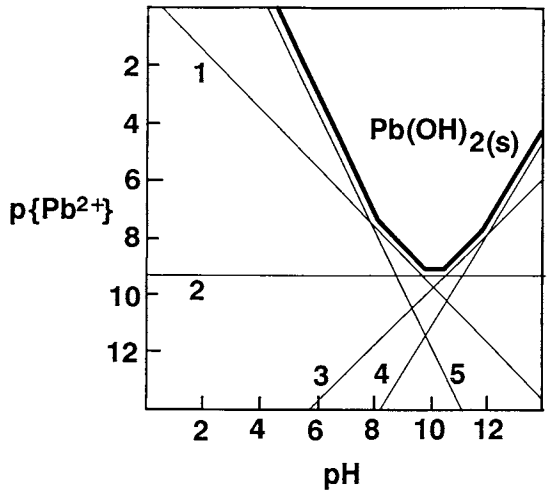

To finish the analysis, we also want to look at how {Pb^{2+}} is in equilibrium with $Pb(OH)_2(s)$. Taking equation (13.49) results in:

$$10^{8.16} = \frac{\{Pb^{2+}\}\{H_2O\}^2}{\{Pb(OH)_2(s)\}\{H^+\}^2} \tag{13.57}$$

Rearranging and solving for {Pb^{2+}} produces:

$$\{Pb^{2+}\} = 10^{8.16}\{H^+\}^2 \tag{13.58}$$

Taking the log of the equation results in:

$$\log\{Pb^{2+}\} = 8.16 - 2pH \tag{13.59}$$

which plots as line 5 in Figure 13.10.

The data in Figure 13.10 are very illustrative. Lead hydroxide shows minimum solubility at about pH 10. By simultaneously solving all the equilibrium expressions for {Pb^{2+}} and {H^+}, it follows that the solid phase is in equilibrium with a number of aqueous species; Pb^{2+} when pH is low (0-8) and OH^- is not abundant (10^{-14} to 10^{-6}M), $Pb(OH)^+$ when pH is near 8 to 10 and OH^- is more abundant (10^{-4} to 10^{-6}M), $Pb(OH)_2^\circ$ at pH 10, $Pb(OH)^{3-}$ at pH 10 to 12 when OH^- is very abundant (10^{-2} to 10^{-4}M) and $Pb(OH)_4^{2-}$ when pH is very high (12 to 14) and OH^- is extremely abundant (10^{-2} to 1.0M). Because $PbOH_2(s)$ is both acid- and base-soluble, this solid phase is considered amphoteric.

Such phenomena are seen with Cd, Zn, Cu, Ni, Co and Hg. The example illustrates how metals exhibit solubility minima when leaching tests are conducted at different pH tests, as shown extensively in Chapter 16.

13.3.6 An Example of Lead Dissolution/Precipitation as $PbCO_3(s)$: The Role of $CO_2(g)$ in Controlling Metal Carbonate Formation

The third simple example expands on the two previous examples. Again, ionic strength effects will be neglected so that activity is synonymous with concentration. Additionally, the role of ligands such as OH^- will be ignored although they could be added to the analysis. In this case, the presence of a constant partial pressure of a gas, $CO_2(g)$, results in the formation of a carbonate solid. Such carbonation or mineralisation reactions are common in incinerator ashes as they age.

$PbCO_3$ (cerrusite) is frequently found in ash residues. Like anglesite, it accounts for some of the available or leachable fraction of lead in combustion residues. Also like anglesite, $PbCO_3(s)$ exhibits a pH-dependent solubility because the conjugate base, CO_3^{2-} (carbonate), can exhibit pH-dependent protonation reactions. However, in the case of carbonate, the source of conjugate base is derived in part from atmospheric $CO_2(g)$ diffusing into a wet alkaline solid. The partial pressure of $CO_2(g)$ can control the amount of carbonate available to precipitate out with lead to form cerrusite.

Frequently, because of biological activity, partial pressures exceed those seen in atmospheric air. This example will be considered as a closed system with an elevated partial pressure and an elevated C_{T,CO_2} of 1×10^{-2}M. In a closed system, such as a large covered ash pile, the uptake of CO_2 from the atmosphere is minimal and the sole source of $CO_2(g)$ is from microbial respiration. Systems open to the atmosphere can also be evaluated.

Consider the following equilibrium reaction:

$$\{PbCO_3(s)\} \rightleftarrows \{Pb^{2+}\} + \{CO_3^{2-}\} \quad \frac{\log K_{sp}}{-13.1} \tag{13.60}$$

Equation (13.60) can be rearranged and put into log form such that:

$$\log\{Pb^{2+}\} = -13.1 - \log\{CO_3^{2-}\} \tag{13.61}$$

Like the anglesite example, it is possible to calculate the activity of CO_3^{-2} as a function of pH for substitution into equation (13.61). The same type of relationship shown in equation (13.44) can be used to calculate $\{CO_3^{2-}\}$; however the appropriate acid dissociation constants have changed ($K_{a,1} = 10^{-6.35}$, $K_{a,2} = 10^{-10.33}$). By selecting various

pH values, the CO_3^{2-} concentration as a function of pH can be determined by substitution into equation (13.61):

pH	$\{H^+\}$	$\{CO_3^{2-}\}$
14	1×10^{-14}	9.99×10^{-3}
12	1×10^{-12}	9.79×10^{-3}
10	1×10^{-10}	3.11×10^{-3}
8	1×10^{-8}	4.55×10^{-5}
6	1×10^{-6}	1.44×10^{-7}
4	1×10^{-2}	4.67×10^{-15}
2	1×10^{-2}	4.67×10^{-15}
0	1×10^{0}	2.08×10^{-19}

If we substitute the log of $\{CO_3^{2-}\}$ into equation (13.61) and solve for $\{Pb^{2+}\}$ we get:

pH	$P\{Pb^{2+}\}$
14	-11.90
12	-11.90
10	-10.59
8	-8.75
6	-6.25
4	-2.41
2	1.23
0	5.58

The values are plotted as a line in Figure 13.11 in a pC-pH plot.

13.3.7 Solubility Control and the Coexistence of Multiple Solid Phases

As discussed earlier, the hypothetical solid phases (Figures 12.3 to 12.6, Chapter 12) show that multiple solid phases can be present initially, possessing differing initial solubilities. Upon initial dissolution, reprecipitation can occur where the secondary mineral has to be in equilibrium with all other solid phases containing the element of interest. Pankow (1991) describes some important solubility laws which are presented below.

Figure 13.11 p{Pb^{2+}} - pH Plot Showing $PbCO_3$(s) in Equilibrium with {Pb^{2+}}

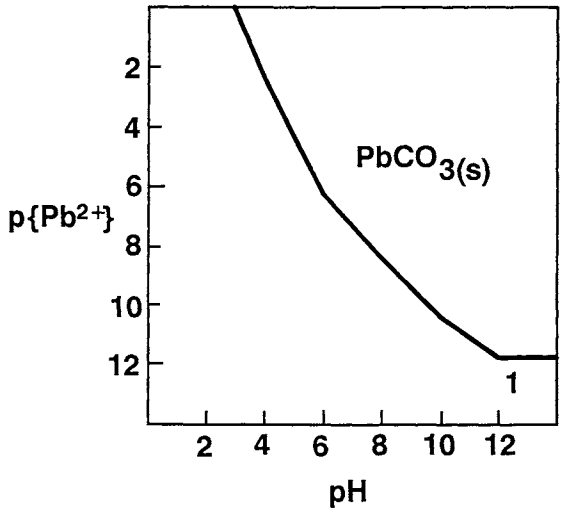

Metals can form solids that are simple salts, hydroxides, oxides, oxyhydroxides, and carbonates. A variety of other types of more complex solid phases are also possible. This is particularly relevant to reprecipitation and secondary mineral formation that occurs during ash leaching. It also seems important to ask if both of these solids could be present and in equilibrium with the same metal ion aqueous activity.

Based on the above discussion, it can be concluded that the criterion for identifying the governing (i.e. the solubility-limiting) solid for a metal ion can be stated using criteria established by Pankow (1991):

Solubility-Limiting Criterion (Pankow, 1991): The solid phase that will limit the solubility of a metal ion will be that which gives the lowest activity of the metal ion at equilibrium for the conditions of interest.

Three corollaries to the above criterion are:

Solubility-Limiting Corollary 1 (Pankow, 1991): If more than one solid is in equilibrium with a given metal ion, then all of those solids must specify the same activity of the metal ion for the conditions of interest.

It may be noted that an analogous situation exists for non-metal containing, anionic species like Cl^-, CO_3^{2-}, etc (Pankow, 1991). That is, the solid that will limit the anion solubility will be the solid which prescribes the lowest equilibrium activity for the conditions of interest (Pankow, 1991). Similarly, if more than one solid is in equilibrium with and controlling a species like sulphate, then all such solids must specify the same activity for that species (Pankow, 1991).

Solubility-Limiting Corollary 2 (Pankow, 1991): If, for the conditions of interest a given solid prescribes a value of the activity of a metal ion that is lower than that prescribed by all other possible solids, then it will also prescribe values for all other dissolved, metal-containing species that are lower than prescribed by all other possible solids for those same conditions.

Just as any given aqueous solution can be characterised by only one value of $\{OH^-\}$ or $\{Cl^-\}$, etc., any given species will be characterised by only one activity coefficient (Pankow, 1991). Thus, the species that prescribes the lowest values of $\{M^{2+}\}$, $\{MOH^{(z-1)+}\}$, $\{M(OH)_2^{(z-2)+}\}$, $\{MCl^{(z-1)+}\}$, etc. will also prescribe the lowest values of $[M^{z+}]$, $[MOH^{(z-1)+}]$, $[M(OH)_2^{(z-2)+}]$, $[MCl^{(z-1)+}]$, etc. and therefore, also the lowest value of the total dissolved metal, $C_{T,M}$ (Pankow, 1991).

Solubility-Limiting Corollary 3 (Pankow, 1991): If a given solid minimises the value of the activity of a metal ion, it will also minimise the total dissolved concentration of $C_{T,M}$; if two solids are coexisting in equilibrium, then they will specify the same value of $C_{T,M}$.

13.3.8 An Example of Lead Dissolution/Precipitation When Both $Pb(OH)_2(s)$ and $PbCO_3(s)$ Are Present

The fourth and final simple example expands on the previous three examples. Again, ionic strength effects and the role of complexing ligands will be ignored for simplicity. In this example, the presence of two solid phases will be examined.

In ash, an element such as lead will be present in a number of mineral phases. However, as pH changes, the relative predominance of any phase can change. There are system pH values where more than one solid phase can stipulate the same activity of Pb^{2+} in solution. Consider the two solids just addressed, $PbSO_2(s)$ and $PbCO_3(s)$.

If we plot on the same graph the solubility plots for $PbSO_4(s)$ ($C_{T,SO_4} = 1x10^{-3}M$) and for $PbCO_3(s)$ ($C_{T,CO_3} = 1x0^{-2}M$), then the plot shown in Figure 13.12 is obtained. At a pH of about 5.20, the two plots intersect. At that pH, both solids specify the same activity for Pb^{2+}. This can be shown mathematically by rearranging and combining equations (13.42) and (13.60) to produce:

$$\{PbCO_{3(s)}\} \rightleftharpoons \{Pb^{2+}\} + \{CO_3^{2-}\} \qquad K_{so} = 10^{-13.1} \qquad (13.62)$$

$$+ \{SO_4^{2-}\} + \{Pb^{2+}\} \rightleftharpoons \{PbSO_{4(s)}\} \qquad 10^{7.79} \qquad (13.63)$$

$$\{SO_4^{2-}\} + \{PbCO_{3(s)}\} \rightleftharpoons \{PbSO_{4(s)}\} + \{CO_3^{2-}\} \qquad 10^{-5.31} \qquad (13.64)$$

The new expression, which takes into account equilibrium constraints from both solids can be modified to produce equation (13.65) (the activities of the solids, by convention, set to equal 1).

$$10^{-5.31} = \frac{\{CO_3^{2-}\}}{\{SO_4^{2-}\}} \qquad (13.65)$$

What the relationship in equation (13.65) is showing is that the two solids will be in equilibrium when the ratio of the activities of the carbonate and sulphate anions in solution at equilibrium is equal to $10^{-5.31}$. Simple trial and error substitution into equation (13.44) for sulphate and its equivalent equation for carbonate show that at about pH = 5.20, the ratio is $10^{-5.31}$.

Figure 13.12 $p\{Pb^{2+}\}$ - pH Plot Showing $PbCO_3(s)$ and $PbSO_4(s)$

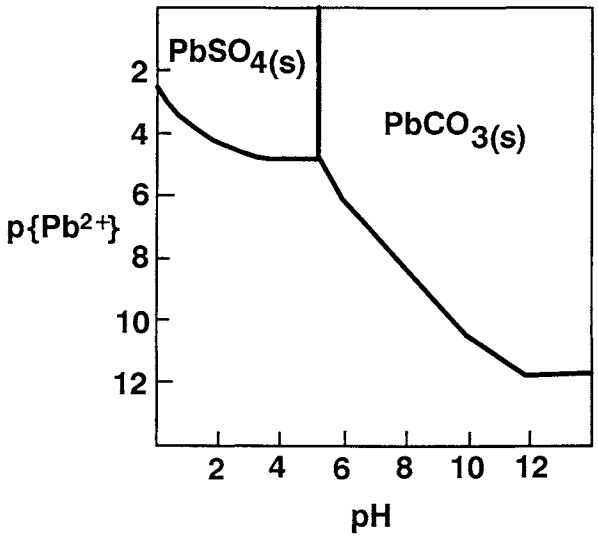

In actuality, ashes contain many solid phases that can undergo incongruent dissolution. For instance, metal carbonates may be present but thermodynamically unstable with respect to a metal hydroxide-governed system. Such incongruence can result in dissolution and reprecipitation in the more thermodynamically-favoured solid phase. While data suggest that ashes do dissolve and reprecipitate (Eighmy et al., 1994), some caution about the application of incongruent dissolution is required. Phases tend to be incompatible with each other only when in intimate contact with each. Thus, heterogeneous mixtures of incompatible phases may remain incompatible only at the local level.

13.3.9 Solid Phase Stability in a Redox-Variable System

The relative oxidising or reducing characteristics of the leaching system plays a crucial role in controlling the types of solid phases that can form. Some of the ashes that are studied are inherently reducing. Certain management scenarios may also cause the deposition environment to become reducing. Therefore understanding such processes becomes important. The principals of redox are used in the modelling efforts described in Chapter 15. These effects are also shown in data presented in Chapter 16.

Many of the scenarios depicted in Figure 12.2, in Chapter 12 for ash leaching scenarios have the opportunity to undergo changes in redox chemistry of the leaching system as a consequence of (i) the presence of bacteria which consume O_2 and cause anoxic, reducing environments to develop, or (ii) the presence of reduced mineral phases in the ash that formed under low O_2 partial pressures in the combustion process. Such mineral phases would include iron-containing minerals where Fe is present as Fe(II) (e.g. $FeCO_3$) or where sulphur is present as S(IV) (e.g. $CaSO_3(s)$), S° (e.g. elemental sulphur) and S(-II) (e.g. PbS).

The role of redox in controlling the predominance of solid phases becomes a function of the type of solid phase that is present and whether or not the solid phase contains a redox-sensitive element. As shown in Figure 13.13 (after Hering and Stumm, 1990), a number of important redox couples exist for elements that can participate in redox reactions. The figure shows the domain of measured pE-pH (or Eh-pH) values seen in natural waters (the shaded area). The dotted lines show the domain where values of pE-pH are likely to exist, but have not been measured, for the redox couples that are known to control redox in the environment. The various solid lines demarcate where an element is in a more oxidised state (above and to the right of the line) or a more reduced state (below and to the left of the line). Additionally, the element in question can undergo changes in valency because it is also redox-sensitive.

A recent review by Hering and Stumm (1990) looked at the mechanisms and rates of oxidative dissolution of reduced phases and reductive dissolution of oxidised phases. Rates are controlled by complex and surface reactions that include transport phenomena to and from the surface of both reactants and products.

Superimposing such solid phase stability issues onto a heterogeneous, multiphase system, it becomes readily apparent that the system becomes increasingly more complex. Regardless of the complexity, this approach is used by geochemists to look at mineral stability in terrestrial systems. The early pioneering work of Pourbaix (1966), Garrels and Christ (1965), and Hem (1967) have laid down the foundation for the construction of Eh (or pE) vs pH stability field diagrams. A more recent effort by Brookins (1988) has resulted in the simple stability fields for almost all the elements of concern to ash chemists. While Brookins prepared the stability fields for use in terrestrial geochemistry systems, they have applicability to the MSW ash leaching system. The methods of Brookins (1988) and Verink (1979) have been used to

construct stability fields for lead in combined ash and scrubber residue. The field is shown in Figure 13.14. Details are provided by Eighmy et al. (1990).

Figure 13.13 A pE - pH Diagram Showing Important Redox Couples and Domains

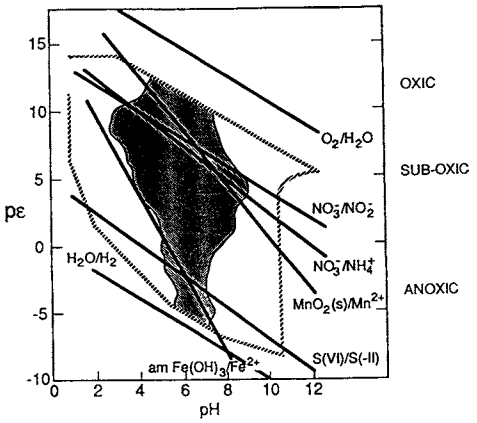

From Hering and Stumm, 1990 with permission from the Mineralogical Society of America

Figure 13.14 An Eh - pH Stability Field Diagram for Lead in Combined Ash and Scrubber Residue

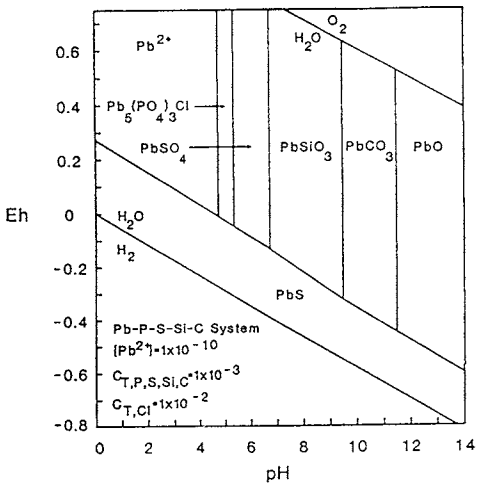

After Eighmy et al., 1990

For a $\{Pb^{2+}\}$ of 1 x 10^{-10}M, predominant phases include PbO, $PbCO_3$, $PbSiO_3$ and $PbSO_4$ under aerobic (oxic) conditions and PbS under reducing conditions. Brookins (1988) and Nriagu (1974) have constructed similar diagrams. Such diagrams are simplistic but helpful in understanding solid phase control. For instance, are these phases seen with speciation methods? Under specific leaching tests, do IAP values suggest that these solid phases control leachability? In modelling these systems, do the geochemical source codes predict that these phases are controlling leaching? By changing the system, can new phases form? These questions get to the very basis of attempts to understand leaching mechanisms.

13.4 CHEMICAL WEATHERING AND AGING

Chemical weathering can be defined as the dissolution of relatively insoluble minerals by the action of water and its solutes (Schnoor, 1990). Until now, this chapter has focused on the dissolution and precipitation (or reprecipitation) of relatively soluble minerals. The more soluble system can be described with a thermodynamic equilibrium approach. Weathering, on the other hand, is better modelled and interpreted mechanistically using a kinetic approach. This approach is postulated because many of the leaching scenarios involving insoluble solid phases such as aluminosilicates will be concerned solely with the forward reaction in dissolution. The backward reaction can be neglected because the solutes are not available in sufficient quantity under appropriate conditions of temperature and pressure to allow the backward reaction to occur.

It is estimated that up to fifty percent of the solid phases in bottom ash are phases that weather like their geological counterparts in metamorphic rock. Many of the discrete solid phases in combustion residues are characterised as iron, magnesium and calcium-containing aluminosilicates or insoluble precipitates/amorphous gels. These phases can comprise a large fraction of the ash particle or solid phase. While their abundance is dependent on the type of residue, the slow dissolution of such phases may have implications under some leaching scenarios where behaviour of this phase is important (i.e. the long term release of lattice-bound or lattice-substituted elements).

Chemical weathering has not been studied in MSW combustion residues. Some work has been done on coal fly ash systems (Warren and Dudas, 1984; 1985; 1986). The majority of the work has been conducted on geologic materials. Reviews by Schnoor (1990), Schott and Petit (1987), Stumm and Weiland (1990), Stumm and Furrer (1987), and Casey and Bunker (1990) are useful, in-depth summaries of dissolution phenomena of these relatively insoluble phases. This brief chapter section is presented as an introduction to the topic. Clearly more work is needed in this area, particularly with regard to evaluating processes for long term leaching applications (e.g. 100 to 1000 years).

13.4.1 The Mineral Surface

At the atomic level, the mineral surface might be conceptualised as shown in Figure 13.15 (Blum and Lasaga, 1987). The surface is three dimensional and contains terraces, steps (or edges), kinks in the edges, and adsorbed atoms (adatoms). The process of solvent interaction with the surface promotes slow dissolution of the surface by the solvent.

Figure 13.15 Mineral Surface

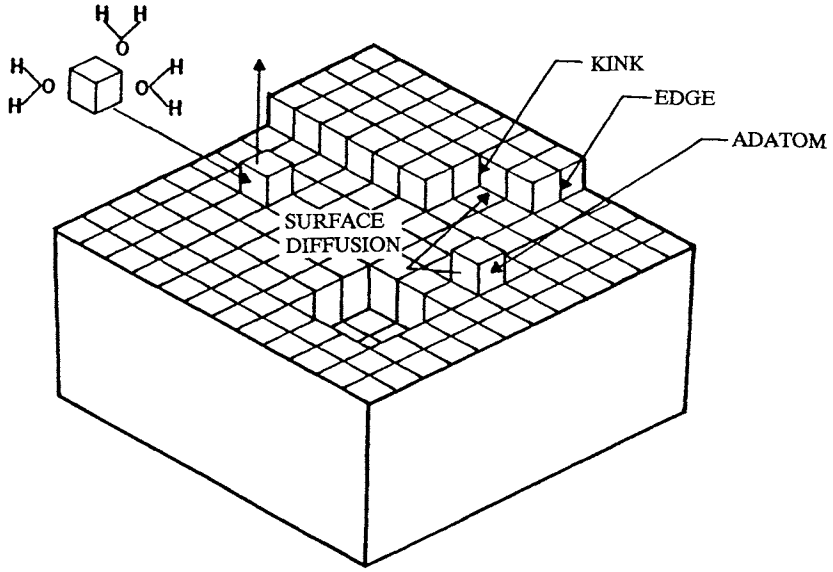

From Blum and Lasaga, 1987. ©1987 John Wiley & Sons, Inc. Reprinted by Permission John Wiley & Sons, Inc

The dissolution of the mineral surface is initiated at sites of high surface energy. These occur at terrace edges, adatoms and kinks at the atomic level and at cracks, scratches or holes in the mineral surface at a larger, sub-micron to micron scale (Schott and Petit, 1987). Ash particles, like geologic materials, have cracks, scratches and holes at the larger scale.

13.4.2 Weathering Reactions

Berner (1978) has visited the issue of rate control of mineral dissolution. Table 13.11 shows a variety of minerals exhibiting high to low solubility. Berner notes that there is a good correlation between the solubility of the mineral and the rate-controlling mechanism for dissolution.

Table 13.11
Dissolution Mechanisms

Mineral	Solubility in Pure Water (moles/L)
Surface Reaction Control	
$KAlSi_3O_8$	3×10^{-7}
$NaAlSi_3O_8$	6×10^{-7}
$BaSO_4$	1×10^{-5}
$SrCO_3$	3×10^{-5}
$CaCO_3$	6×10^{-5}
Ag_2CrO_4	1×10^{-4}
$SrSO_4$	9×10^{-4}
Opaline SiO_2	2×10^{-3}
Mixed Control	
$PbSO_4$	1×10^{-4}
Transport Control	
AgCl	1×10^{-5}
$Ba(IO_3)_2$	8×10^{-4}
$CaSO_4 \cdot 2H_2O$	5×10^{-3}
$Na_2SO_4 \cdot 10H_2O$	2×10^{-1}
$MgSO_4 \cdot 7H_2O$	3×10^{0}
$Na_2CO_3 \cdot 10H_2O$	3×10^{0}
KCl	4×10^{0}
NaCl	5×10^{0}
$MgCl_2 \cdot 6H_2O$	5×10^{0}

Adapted from Berner, 1978 reprinted with permission of the American Journal of Science

Three domains are described. The first is the transport control domain where dissolution is so fast that the ability of the dissolved solute to diffuse out of the depleted surface of the mineral or out of the diffusion boundary layer around the particle rate limits dissolution. The second is the surface reaction control domain, where dissolution kinetics are so slow compared to diffusional transport that dissolution is the rate-controller. The third domain is a mixture of the two processes.

13.4.3 Surface Reaction-Controlled Dissolution

The dissolution mechanism that occurs at the mineral-water interface involves a number of reactants. These include the components of water, H_2O, H^+ and OH^-, as well as the ligands present in the leaching solution. The slow, kinetically-constrained dissolution involves both chemical and physical reaction steps. These steps are: the attachment of reactants at reaction sites where they polarise and weaken metal-oxygen bonds in the mineral lattice and the rate limiting detachment of surface metal species. This two-step reaction is depicted as follows (Stumm and Furrer, 1987):

I. Surface (adatoms, edges, kinks) + (H^+, HO^-) + reactants	fast ——> (<----)	Activated surface species
II. Surface detachment of activated species	slow ——> (<----)	Aqueous metal ion

For the two-step reaction, backward reaction arrows are shown. When initial surface sites are consumed and new sites are created, steady state conditions can develop. Finally, if the system is far from equilibrium or if equilibrium is unattainable in the leaching system under consideration, then the back reactions can be assumed to be negligible and the dissolution rate becomes (Stumm and Furrer, 1987):

$$\text{Dissolution Rate} \propto \left(\begin{array}{c}\text{Reactant Concentration}\\ \text{at the Surface}\end{array}\right) \times \left(\begin{array}{c}\text{Density of}\\ \text{Surface Sites}\end{array}\right)^n$$

where n is the number of mobile, solvent phase reactants required to activate the metal ion at the reaction site. The higher the surface energy at the reaction site, the faster the rate of dissolution.

Dissolution may initially be incongruent. Basic cations such as Ca^{2+}, Mg^{2+}, Na^+, K^+ may preferentially dissolve before Al^{3+} and Si^{4+}. Subsequent dissolution then becomes congruent when all elements are removed at the same rate (Schnoor, 1990).

Weiland et al. (1988) have developed a model to describe surface reaction controlled dissolution. The rate law is:

$$R = kX_aP_jS_{sites} \qquad (13.66)$$

where

R is the proton or ligand-promoted dissolution rate (mol m^{-2} s^{-1}),
k is the rate constant (s^{-1}),
X_a is the mole fraction of reaction sites (dimensionless),
P_j is the probability of a finding a site for an activated precursor complex,
S_{sites} is the total surface concentration of sites (mol m^{-2}).

Schnoor (1990) provides a detailed description of a surface reaction-controlled dissolution reaction. The surfaces of oxides and aluminosilicate minerals in the presence of water are characterised by amphoteric surface hydroxyl groups. The surface OH^- group has a complex-forming O-donor atom that coordinates with H^+ and metal ions (Kummert and Stumm, 1980; Sigg and Stumm, 1981). The underlying aluminum or metal ion in the surface tetrahedra of the mineral and other cations are subject to coordination with OH^- groups, which, in turn, weakens the bond to their structural oxygen atoms. Detachment of an activated complex removes the coordination complex and renews the surface for further hydrolysis, protonation and dissolution. An example of hydrolysis, protonation, formation of the surface coordination complex and detachment to solution is shown in Figure 13.16 for an aluminum oxide.

Figure 13.16 Dissolution of an Aluminum Oxide Surface

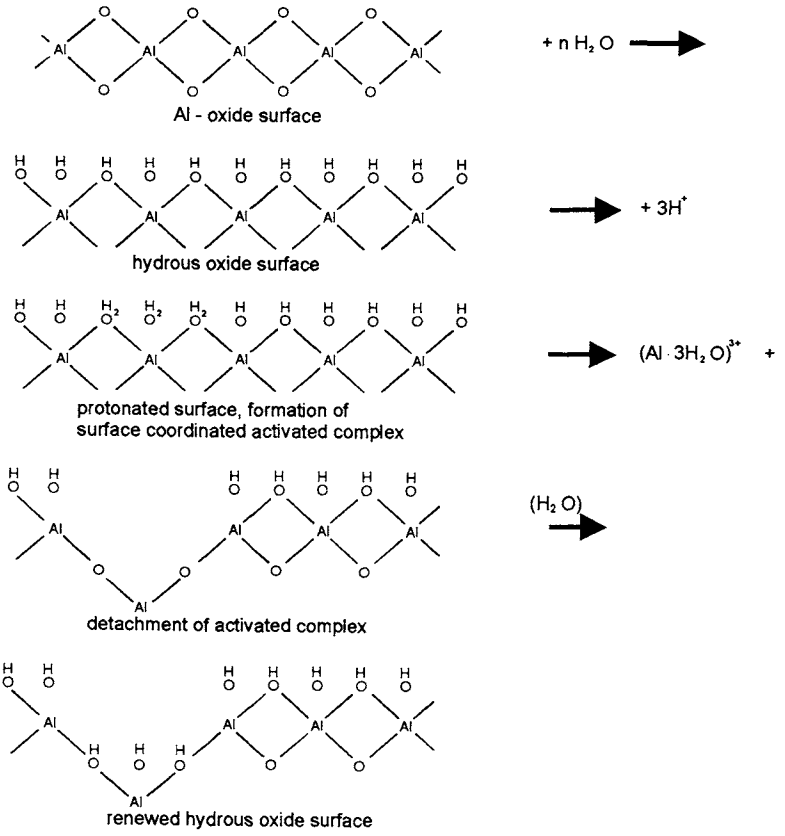

Schoor, 1990. ©1990 John Wiley & Sons, Inc. Reprinted by permission John Wiley & Sons, Inc.

A very important result of recent laboratory studies has been the fractional order dependence of mineral dissolution on solution phase hydrogen ion activity. If the dissolution reaction is controlled by hydrogen ion diffusion through a boundary layer, a first-order dependence on $\{H^+\}$ would be expected. If the dissolution reaction is governed by some other factor like surface area, then the dependence on hydrogen ion activity should be zero-order. Rather, the dependence exhibits a fractional order for a wide variety of minerals, indicating a surface reaction controlled dissolution (Schott et al., 1981; Giovanoli, et al. 1989; Schnoor and Stumm, 1986; Busenberg and Plummer, 1982; Grandstaff, 1977; Furuichi et al., 1969).

A strong dependency on the dissolution rate can be seen. Wollast and Chou (1985) have looked at the dissolution of silica from various mineral phases; minimal releases are seen at pH 3.0. This pH corresponds to the zero point of charge (ZPC), or pH condition where the negative site density of adsorbed OH^- equals the positive site density of adsorbed H^+. Relative protonation or hydroxylation enhances site activation.

13.4.4 Weathering Rates

There is quite a lot of data available on dissolution rates of minerals. While these rates have not yet been formally established for MSW residues, it is likely that similar rates will be shown. Table 13.12 summarises a few data (Schnoor, 1990) for silicon release from a variety of silicon-containing minerals. The rates of Si dissolution are all similar: approximately 5×10^{-12} moles per cm^2 per second.

Table 13.12
Measured Weathering Rates

Mineral	Weathering Rate (mol Si m^{-2} s^{-1})
Plagioclase (oligoclase)	5×10^{-12}
Plagioclase (bytownite)	5×10^{-12}
Olivine	7×10^{-12}
Plagioclase, biotite	6×10^{-12}

Adapted from Schnoor, 1990.

There are no direct data available on the weathering rates of glassy phases in various combustion residues. There are mineral phases in bottom ash, e.g. fine-grained quartz and feldspars, that will undergo weathering reactions according to models adopted by Berner (1981). A cursory examination of silicon leaching rates from bottom ash for a variety of less aggressive leaching tests shows that silicon leaching rates can range

from 5×10^{-13} to 5×10^{-10} moles per cm^2 per second. These values fall within the same magnitude as those reported by Schnoor (1990). This suggests that silicon leaching is probably a kinetically slow weathering-like reaction in bottom ash.

13.4.5 Aging Reactions

There are a number of aging reactions that can occur in hydrated ash specimens over time. The aging reactions are diagenetic in nature; the residue becomes more "rock-like" in its mineralogy and phase compatibility. The underlying processes that cause aging are the thermodynamic instability of, or incongruence between, mineral phases. The slow, irreversible conversion to more stable phases is the process that corrects the instability.

There are at least six processes that occur during aging reactions:

(i) the oxidation of elemental metals to oxides,
(ii) the hydrolysis of oxides and liberation of exothermic heat,
(iii) the uptake of carbon dioxide and the subsequent formation of carbonate-containing minerals,
(iv) the redox-driven oxidation of elemental metals (notably Al°) and reduction of water to generate hydrogen gas,
(v) the formation of certain mineral phases in bottom ashes that act as pozzolans for particle aggregation and strength development, and
(vi) the formation of clay-like phases in residues.

The oxidation of elemental metals to form metal oxides is a small, but not insignificant aging reaction that can occur in all residues. An example would be the conversion of elemental iron to iron oxides. The following reactions depict the conversion of ferric iron to various iron oxides found in bottom ash:

$$Fe^{3+} + 3/2\ H_2O \rightleftharpoons \frac{1}{2}\ \alpha\text{-}Fe_2O_3(\text{hematite}) + 3H^+ \qquad (13.67)$$

$$Fe^{3+} + 2\ H_2O \rightleftharpoons \alpha\text{-}FeOOH(\text{goethite}) + 3H^+ \qquad (13.68)$$

Goethite is the most stable and least soluble form of iron oxide in oxidised systems (Schwertmann and Taylor, 1977). Hematite will convert to goethite via the following reaction:

$$Fe_2O_3 + H_2O \rightleftharpoons 2\alpha\text{-}FeOOH \qquad (13.69)$$

The hydrolysis of metal oxides can be an aging reaction that releases substantial quantities of heat. An example reaction is the conversion of an oxide to a hydroxide:

$$CaO + H_2O \leftrightarrows Ca(OH)_2 \quad (13.70)$$

This reaction, which may occur when APC residues are wetted, tends to release 400 to 500 joules of heat for every kilogram of CaO that is hydrolysed (Boynton, 1980).

The uptake of $CO_2(g)$ from the atmosphere into alkaline residues is another significant aging reaction. Many hydroxide phases can be converted to carbonate phases as shown in the following reactions:

$$Ca(OH)_2 + CO_2 \leftrightarrows CaCO_3 + H_2O \quad (13.71)$$

$$CaCO_3 + CO_2 + H_2O \leftrightarrows Ca(HCO_3)_2 \quad (13.72)$$

Kluge et al. (1980) have studied the redox reactions occurring during ash aging that result in the release of hydrogen gas. The most likely reaction involves elemental aluminum under alkaline conditions:

$$2\ Al^\circ + 6H_2O \leftrightarrows 2\ Al(OH)_3(s) + 3H_2(g) \quad (13.73)$$

Kluge (1980) was able to quantify hydrogen gas release from bottom ash used as road base. Hydrogen gas is probably evolved when bottom ash is quenched.

Oberste-Padtberg and Schweden (1990) have measured H_2 release under alkaline conditions when fly ash is stabilised with Portland cement. They also quantified methane and carbon monoxide evolution. The reaction for methane evolution was hypothesised to involve metal carbides which are found in the residues:

$$Me_4C_3 + 6H_2O \rightarrow Me_2O_3 + 4CH_4 \quad (13.74)$$

The next important aging reaction involves the formation of certain mineral phases associated with pozzolanic reactions. Such reactions can change leaching behaviour by altering particle-specific surface areas and reducing porosity. Such reactions have not been extensively studied in bottom ashes. Van der Wegen (1991) has found ettringite ($3CaO{\bullet}Al_2O_3{\bullet}3CaSO_4{\bullet}32H_2O$) in aged bottom ash specimens. SEM and XRPD were used to detect the mineral phase. Ettringite, formed from gypsum ($CaSO_4{\bullet}2H_2O$) and tricalcium aluminate ($Ca_3Al_2O_6$), is an important initial phase in the cementation process. Stämpfli (1992) identified gypsum in aged bottom ash. He was

not able to find tricalcium aluminate or the calcium silicates (Ca_3SiO_5 or Ca_2SiO_4) that are needed to complete the pozzolanic cementation process despite the monolithic nature of the sample.

The last aging reaction to be identified is the weathering of glassy phases in bottom ash to form clay-like crystal lattice structures. Zevenbergen et al. (1993) obtained bottom ash from a 12-year old disposal site. A variety of analytical techniques were used to identify the clay-like structure.

There are undoubtedly many other aging phenomena that have not been identified. As more researchers investigate these processes, more aging and weathering reactions will be identified.

13.5 SORPTION

The solid phase in the ash leaching system (Figure 12.2, Chapter 12) can also play an important role in controlling the appearance and disappearance of solutes in the leaching solution through the process of sorption/desorption. Like precipitation/dissolution and solution-phase complexation, sorption is usually an equilibrium reaction. Many field and laboratory leaching data must be interpreted with sorption as another equilibrium process that must be simultaneously solved with other equilibrium expressions. Sorption plays an important role in the fine-tuning of modelling efforts introduced in Chapter 15.

Most ash residues contain a number of metal oxides. These mineral phases include anatase (TiO_2), corundum (α-Al_2O_3), magnetite (Fe_3O_4), rutile (TiO_2) and quartz (α-SiO_2). Such mineral phases, as well as others that are present in combustion residues, constitute the sorptive surfaces in ash.

The thermodynamics and modelling of sorption to mineral surfaces is complex. The following section provides a brief introduction to the topic. Adsorption processes undoubtedly play an important role in controlling metal leaching. However, the process has not been well studied in residues. The reader is encouraged to review the works of Sposito (1984), Leckie (1988), Sigg (1987), Schindler and Stumm (1987), Parks (1990) and Davis and Kent (1990). As research continues into a mechanistic understanding of leaching, it is anticipated this topic will become more important to understanding and modelling leaching behaviour.

13.5.1 Surface Functional Groups

Metal oxides and hydroxides are surfaces where adsorption reactions take place. Oxides that become hydrated possess proton-bearing surface functional groups that can disassociate at high pH or reassociate at low pH. Aluminosilicate mineral phases

that do not have isomorphic substitutions, or substituted atoms in the crystal lattice, also can develop hydrated proton-bearing surface functional groups.

As shown in Figure 13.17, surface hydroxyl groups comprise the functional groups on a variety of oxide and aluminosilicate mineral surfaces. Various types of surface hydroxyl groups are shown. The M (metal) and O (oxygen) function groups at the surface exhibit negative charge distributions that cause H_2O to "chemisorb" to form surface hydroxyl groups. The chemisorption process usually involves a loss of a proton from the water molecule. Hydrogen bonding between the surface hydroxyl groups and either water vapour or liquid water causes layers of water to physically adsorb to the surface (Davis and Kent, 1990). These hydroxyl functional groups have different reactivities (Sposito, 1984); some hydroxyl groups dissociate easily to form the anionic oxygen ligand, other hydroxyl groups dissociate less easily. Another type of site that can develop is a Lewis Acid site (Davis and Kent, 1990). In such a site, H_2O chemisorbs directly to a bare metal ion. In this case the site can only act as a proton donor.

Figure 13.17 Different Types of Mineral Surface Hydroxyl Groups

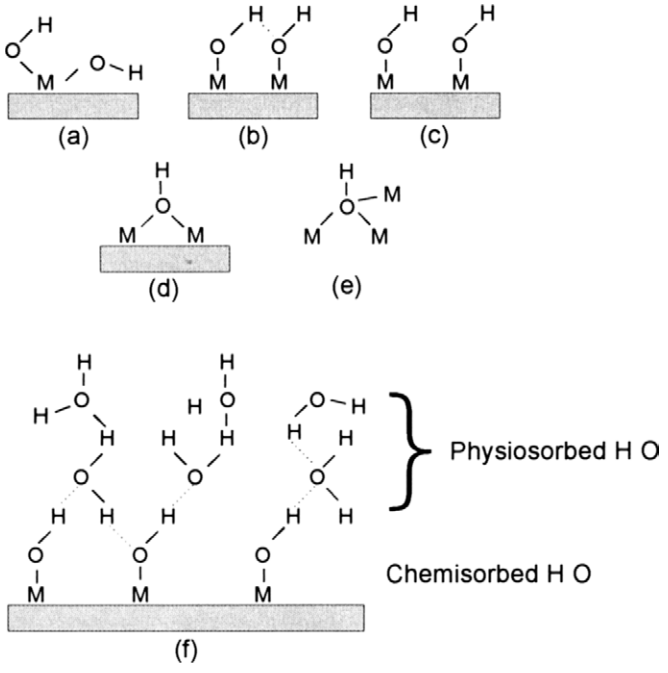

From Davis and Kent, 1990 with permission from the Mineralogical Society of America

Table 13.13 provides some information on hydroxyl site densities for various minerals. Values range from 1.3 to 22 functional groups per nm^2. Goethite, a particularly adsorptive iron oxide (α-FeOOH) that is also a principal mineral phase in bottom ash, exhibits different numbers of adsorption sites depending upon the adsorbing cation (Table 13.14).

Table 13.13
Density of Surface Functional Groups on Various Oxide and Hydrous Oxide Minerals

Mineral	Range of Site Densities (sites nm^{-2})
Goethite (α-FeOOH)	2.6-16.8
α-Fe_2O_3	5-22
Rutile (TiO_2)	12.2
Gibbsite (α-$Al(OH)_3$)	2-12
γ-Al_2O_3	6-9
SiO_2 (Quartz)	4.5-12
Kaolinite	1.3-3.4

Adapted from Davies and Kent, 1990 with permission from the Mineralogical Society of America

Table 13.14
Site Densities on Goethite (α-FeOOH)

Adsorbing Ion	Adsorption Maximum (sites nm^{-2})
OH^-/H^+	4
OH^-	2.6
F^-	5.2 - 7.3
SeO_3^{2-}	1.5
PO_4^{3-}	0.8
Pb^{2+}	2.6 - 7.0

Adapted from Davies and Kent, 1990 with permission from the Mineralogical Society of America

The surface functional groups exhibit acid-base behaviour; they can donate or receive protons. The pH at which the mineral exhibits no net charge (or "zero point charge") in an electric field, the pH_{zpc}, is useful in understanding at what pH mineral surfaces exhibit tendencies to adsorb solutes of opposite charge. At a pH < pH_{zpc}, the surface would adsorb anions. At pH > pH_{zpc}, the surface would adsorb cations. Table 13.15 depicts some pH_{zpc} for various adsorbent mineral phases.

Sorption phenomena are usually modelled using empirical, experimentally determined sorption constants based on solute activity or using mechanistic explanations of the electrostatic interactions that occur at the particle surface. Both approaches can be modelled in the modelling programs described in Chapter 15.

Table 13.15
Estimates of pH_{pze} for Various Minerals

Mineral	pH_{pzc}
γ-Al_2O_3	8.5
Anatase (T_iO_2)	5.8
Birnessite (δ-MnO_2)	2.2
Calcite ($CaCO_3$)	9.5
Corundum (α-Al_2O_3)	9.1
Goethite (α-FeOOH)	7.3
Hematite (α-Fe_2O_3)	8.5
Magnetite (α-Fe_3O_4)	6.6
Rutile (TiO_2)	5.8
Quartz (α-SiO_2)	2.9

Adapted from Davis and Kent, 1990 with permission from the Mineralogical Society of America

13.5.2 Activity-Based Sorption Models

The first activity-based sorption model is based on the distribution coefficient, K_d (Allison et al., 1990). Using the convention of M as a metal and SOH as a hydroxylated surface sorption site, consider the following reaction depicting m sorbing to the surface site:

$$SOH + M \rightleftharpoons SOH \cdot M \tag{13.75}$$

The ratio of sorbed metal concentration to the total analytical metal concentration in solution at equilibrium is the distribution coefficient. It is analogous to an equilibrium constant:

$$K_d = \frac{[SOH \cdot M]}{[M]} \tag{13.76}$$

It is more appropriate to examine the K_d relationship based on the activity of participating aqueous metal solute:

$$K_d^{act} = \frac{\{SOH \cdot M\}}{\{M\}} \tag{13.77}$$

By convention [SOH • M] = {SOH • M} and equation (13.77) becomes:

$$K_d^{act} = \frac{[SOH \cdot M]}{\gamma_m [M]} \tag{13.78}$$

Many K_d^{act} values are tabulated in the sorption review document prepared by Rai and Zachara (1984).

The second approach that employs activity in an empirical way to depict sorption is the Langmuir adsorption model (Allison et al., 1990). Again, using the SOH and M terminology, consider the following reaction:

$$SOH + M \rightleftharpoons SOH \cdot M \tag{13.79}$$

where at equilibrium

$$K_L^{act} = \frac{\{SOH \cdot M\}}{\{M\}\ \{SOH\}} \tag{13.80}$$

Conventionally, the Langmuir constant is derived experimentally using various quantities of SOH and M. To place K_L^{act} into the more familiar context of the Langmuir adsorption isotherm, a mass balance on surface sites is needed (Allison et al., 1990):

$$[SOH]_T = [SOH \cdot M] + [SOH] \tag{13.81}$$

Combining equations (13.80) and (13.81) produces:

$$[SOH \cdot M] = \frac{K_L^{act}\ [SOH]_T\ \gamma_M[M]}{1 + K_L^{act}\ \gamma_M[M]} \tag{13.82}$$

The only difference between K_d^{act} and K_L^{act} is that the Langmuir equation assumes a finite concentration of SOH. Values for K_L^{act} can be found in Rai and Zacchara (1984).

The third activity-based empirical sorption model is the Freundlich model (Allison et al., 1990). Again using the SOH and M terminology, consider the following reaction:

$$SOH + 1/nM \rightleftharpoons SOH \cdot M \tag{13.83}$$

where at equilibrium

$$K_f^{act} = \frac{\{SOH \cdot M\}}{\{M\}^{1/n}\{SOH\}} \tag{13.84}$$

Imposing the convention that {SOH • M} = [SOH • M], equation (13.84) becomes:

$$[SOH \cdot M] = K_f^{act}\{M^{M+}\}^{1/n} \tag{13.85}$$

The 1/n term is a mass action stoichiometric coefficient related to M. K_f^{act} is similar to K_d^{act} if n=1. K_f^{act} differs from K_L^{act} in its implicit assumptions about an unlimited supply of unreacted surface sites at equilibrium. K_f^{act} values can be found in Rai and Zacchara (1984).

The fourth empirical, activity-based sorption model is the ion exchange model (Allison et al, 1990). Again using the SOH terminology, but denoting the exchangeable metal as M and the sorbing metal as M_2, consider the following:

$$SOH \cdot M_1 - M_1 + M_2 \rightleftharpoons SOH \cdot M_2 \tag{13.86}$$

where at equilibrium,

$$K_{ex} = \frac{\{M_1\}\{SOH \cdot M_2\}}{\{M_2\}\{SOH \cdot M_1\}} \tag{13.87}$$

K_{ex} differs from the other three constants by assuming a substitution reaction occurs at SOH. K_{ex} values are found in Rai and Zacchara (1984).

There are no conventions as to the applicability of these four empirical models (Allison et al., 1990). When modelling sorption processes, all four models can be tested (provided appropriate constants are available). The literature does suggest that mechanistic models based on electrostatic considerations do a better job at modelling sorption (Allison et al., 1990); frequently parameters for these models are not available (as discussed below).

13.5.3 Electrostatic Surface Complexation Models

There have been a number of attempts to model adsorption to mineral surfaces while taking into account electrostatic interactions between charged surfaces and solutes. The models explain how both cations and anions adsorb as a function of pH, adsorbent site density and ionic strength (Westall and Hohl, 1980). Models such as the constance capacitance model (CCM) and the diffuse double layer model (DLM) were developed (Davis and Kent, 1990). A third model, the triple layer model (TLM), was developed to have multiple adsorption planes on the mineral surface to allow for outer sphere as well as inner sphere complexes to form (Leckie, 1988). The TLM is viewed as most applicable and is presented here.

The TLM is schematically depicted in Figure 13.18 (Leckie, 1988). As described by Evans (1989), tightly bound inner sphere complexes reside in the inner or surface plane, λ_{is} (or α plane). Outer sphere complexes reside in the adjacent plane, λ_{os} (or β plane). Noncomplexed species reside in the diffuse layer, λ_d (or d plane). To maintain electroneutrality, the charge density, σ, must equal the intrinsic charge density of the mineral such that:

$$\sigma_{int} + \sigma_{is} + \sigma_{os} + \sigma_d = 0 \qquad (13.88)$$

Figure 13.18 Depiction of the Triple Layer Model

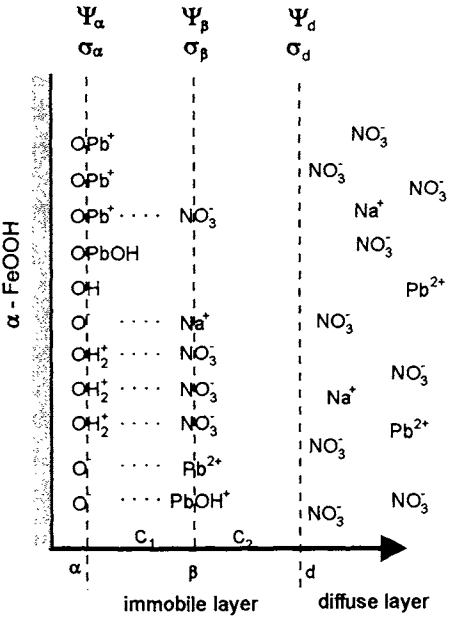

Reprinted with permission from Leckie, 1988. Copyright Lewis Publishers, an imprint of CRC Press, Boca Raton, Florida. ©1988

Hayes (1987) has depicted the types of binding mechanisms that can occur in both the inner and outer spheres (Figure 13.19). The figure shows various inner sphere and outer sphere complexation reactions that can occur.

Figure 13.19 Schematic Depiction of Coordinative Surface Complexes and Ion Pairs at Oxide Surfaces

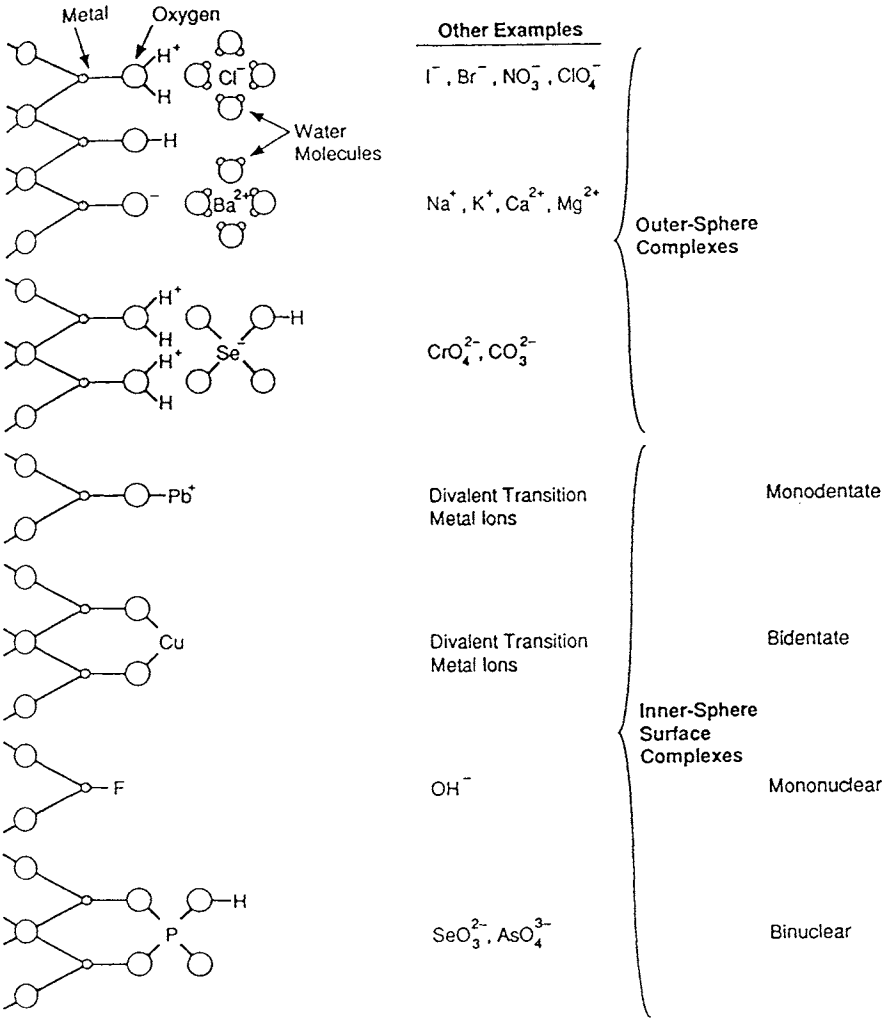

From Hayes, 1987 with permission of the author

Consider the following reaction for the monovalent metal ion M^+ (Allison et al., 1990):

$$SOH - H_s^+ + M_s^+ \rightleftarrows (SO \cdot M) \tag{13.89}$$

where SOH and M_s^+ are the same surface binding site and sorbing metal and H_s^+ is the sorbed proton that must deprotonate from SOH to allow for formation of the sorbed complex SO • M.

By convention,

$$\{H_s^+\} = \{H^+\} [e^{-\psi_o F/RT}] \tag{13.90}$$

and

$$\{m_s^+\} = \{m^+\} [e^{-\gamma_\beta F/RT}] \tag{13.91}$$

where $e^{-\psi F/RT}$ is the Boltzmann factor for either the α or β planes depicted in Figure 13.19. Equations (13.86) through (13.88) can be written as an equilibrium expression (Allison et al., 1990):

$$K = \frac{\{SO \cdot M\} \{H^+\} [e^{-\psi_o F/RT}]}{\{SOH\} \{M^+\} [e^{-\psi_\beta F/RT}]} \tag{13.92}$$

Other forms of equation (13.89) can be provided for a hydrolysis reaction of the type (Allison et al., 1990):

$$SOH + M_s^{2+} + H_2O - 2H_s^+ \rightleftarrows SO \cdot MOH \tag{13.93}$$

producing,

$$K = \frac{\{SO \cdot MOH\} \{H^+\}^2 [e^{-\psi_o F/RT}]^2}{\{SOH\} \{M^{2+}\} \{H_2O\} [e^{-\psi_\beta F/RT}]^2} \tag{13.94}$$

A similar approach can be taken for a sorbing monovalent anion (Allison et al., 1990):

$$SOH + A_s^- + H_s^+ \rightleftarrows SOH_2 \cdot A \tag{13.95}$$

producing,

$$K = \frac{\{SOH_2 \cdot A\} [e^{-\psi_\beta F/RT}]}{\{SOH\} \{A^-\} \{H^+\} [e^{-\psi_o F/RT}]} \tag{13.96}$$

Finally, a similar approach can be taken for a sorbing divalent anion (Allison et al., 1990):

$$SOH + A_s^{2-} + H_s^+ \rightleftharpoons SOH_2 \cdot A \tag{13.97}$$

producing

$$K = \frac{\{SOH_2 \cdot A^-\}\,[e^{-\psi_\beta F/RT}]^2}{\{SOH\}\,\{A^{2-}\}\,\{H^+\}\,[e^{-\psi_o F/RT}]} \tag{13.98}$$

The geochemical model MINTEQA2 has the capability to model sorption using estimated parameters for the TLM as well as the CCM and DLM.

The TLM model has been widely used to model adsorption of cations and anions (Davis and Kent, 1990). For adsorption to oxides, Davis and Leckie (1978, 1980), Balistrieri and Murray (1982), Hsi and Langmuir (1985), Catts and Langmuir (1986), LaFlamme and Murray (1987), Zachara et al. (1987), Hunter et al. (1988), and Zachara et al. (1987) have successfully used the model. It has also been applied to non-hydrous oxide minerals like quartz, titanium and clay (Shuman, 1986).

13.5.4 Adsorption Data

Davis and Kent (1990) have compiled some interesting data as to how cations and anions adsorb to mineral surfaces. As shown in Figure 13.20, there is a narrow pH range where a cation or anion goes from near zero adsorption to high levels of adsorption. This adsorption edge occurs at pH_{ads}, the pH where significant sorption occurs, which is close to the pH_{zpc}. Cations adsorb at high pH by forming inner sphere complexes with the deprotonated hydroxyl functional groups. Anions adsorb at low pH when forming inner sphere complexes with protonated functional groups.

13.6 A UNIFIED APPROACH TO LEACHING

The information compiled in this chapter allows us to assemble an approach to characterising the leaching process.

Understanding fundamental leaching behaviour of a residue such as ash requires the consideration of many factors (Figure 13.21). The speciation of the elements in the solid phase plays a fundamental role in controlling the nature of the leachate. This can then be related to that fraction of an element that is available for leaching. Particle morphology, porosity, and diffusion pathlength are also critical in assessing the role of diffusion in controlling reactions. Attempts to characterise those leaching processes that are kinetically based or thermodynamically based is an additional approach that is needed. The thermodynamic mechanisms can be modelled with geochemical codes. Additional data can be gleaned by conducting leaching studies to assess the effects

of pH, E_h and ligands on dissolution phenomena. The processes surrounding sorption cannot be ignored; these studies can be compared to the various sorption models that are presently available. Finally, the role of the L/S ratio and time must be considered.

Figure 13.20 Adsorption Edges for Various Cations and Anions

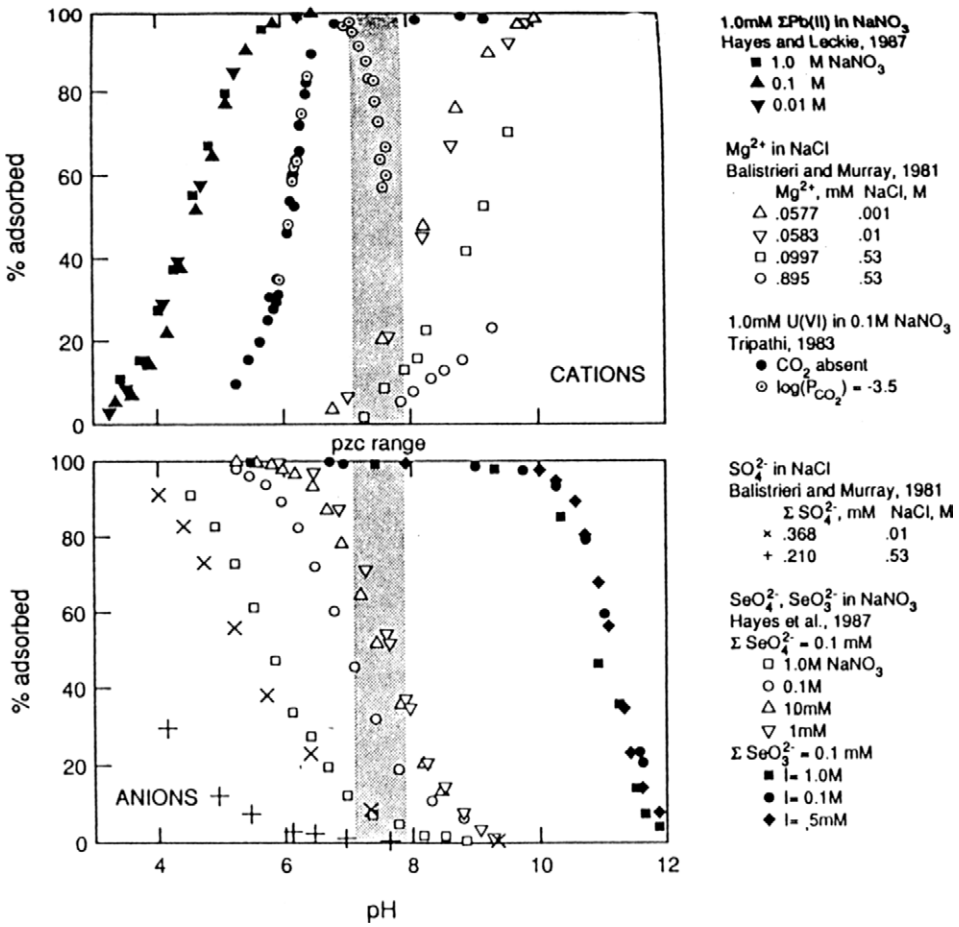

From Parks, 1990 with permission of the Mineralogical Society of America

Now that these concepts have been explained, they need to be applied. The next chapter sets out various types of leaching tests which can be performed to determine certain characteristics of ash under specific sets of leaching conditions.

Figure 13.21 Schematic of Fundamental Leaching Behaviour

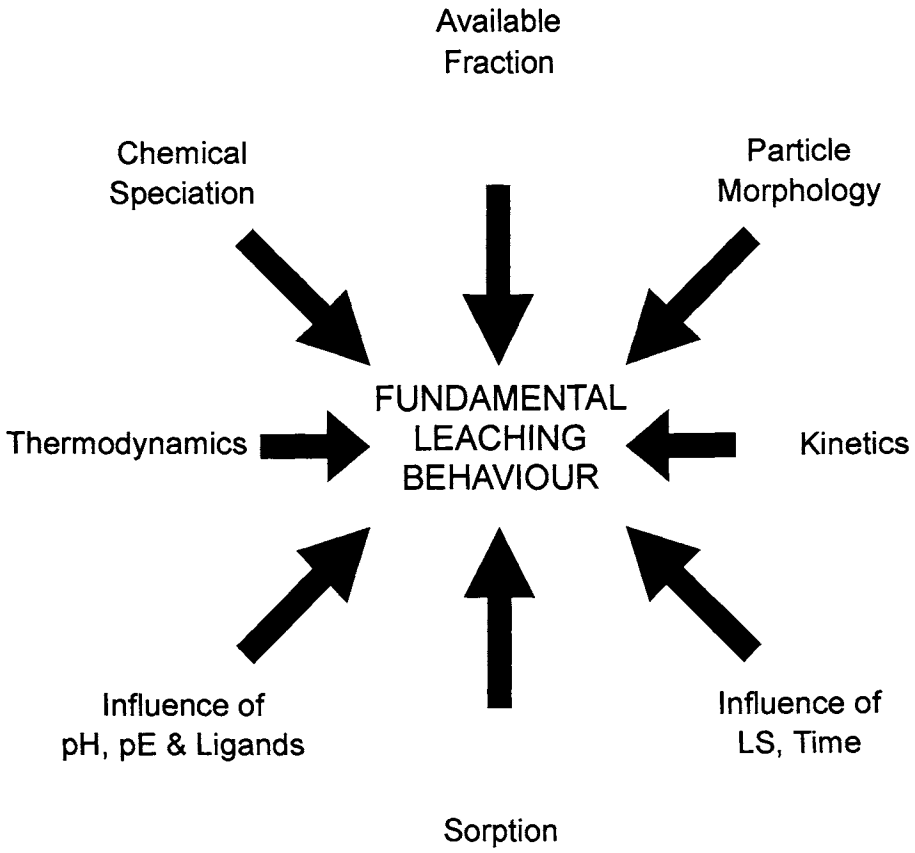

REFERENCES

Allison, J.D., D.S. Brown and K.J. Novo-Gradac. MINTEQA2/PRODEFA2, A Geochemical Assessment Model for Environmental Systems: Version 3.0 User's Manual. Environmental Research Laboratory, U.S. EPA, Athens, GA, 1990.

Baes, C.F. and R.E. Mesmer. The Hydrolysis of Cations. John Wiley & Sons, New York, 1976.

Balistrieri, S.L. and J.W. Murray. The Adsorption of Cu, Pb, Zn, and Cd on Goethite from Major Ion Seawater. Geochim. Cosmochim. Acta 46, pp. 1253-1265, 1982.

Belevi, H. and P. Baccini. Long-Term Assessment of Bottom Ash Monofill Leachates. In Proceedings of the International Conference on Municipal Solid Waste Combustion. April 11-14, Hollywood, FL, USA, 1989.

Berner, R.A. Rate Control Of Mineral Dissolution Under Earth Surface Conditions. Am. J. Sci. 278, pp. 1235-1252, 1978.

Berner, R.A. Kinetics of Weathering and Diagenesis. In Kinetics of Geochemical Processes (A.C. Edited by A.C. Lasaga and R.J. Kirkpatrick. Mineralogical Society of America, Washington, D.C., p. 111, 1981.

Blum, P.J. and A.C. Lasaga. Monte Carlo Simulations of Surface Reaction Rate Laws. In Aquatic Surface Chemistry: Chemical Processes at the Particle-Water Interface Edited by W. Stumm. John Wiley and Sons, NY, p. 255, 1987.

Boynton, R.S. Chemistry and Technology of Lime and Limestone. John Wiley and Sons, NY, 1990.

Brookins, D.G. Eh-pH Diagrams for Geochemistry. Springer-Verlag, Berlin, 1988.

Busenberg, E. and A.B. Plummer. The Kinetics of Dissolution of Dolomite in CO_2-H_2O Systems at 1.5 to 65°C and 0 to 1 atm pCO_2. Am. J. Sci. 282, pp. 45-78, 1982.

Butler, J.N. Solubility and pH Calculations. Addison-Wesley, Reading, MA, 1964.

Casey, A.B. and A.B. Bunker. Leaching of Mineral and Glass Surfaces. In Mineral-Water Interface Geochemistry Edited by M.F. Hochella, Jr. and A.F. White. Mineralogical Society of America, Washington, D.C., p. 397, 1990.

Catts, A.B. and A.B. Langmuir. Adsorption of Cu, Pb and Zn onto birnessite (δ-MnO_2). J. Appl. Geochim 1, pp. 255-264, 1986.

Cole, D.R. Theory and Application of Adsorption and Ion Exchange Reaction Kinetics to in situ Leaching of Ores. In Leaching and Diffusion in Rocks and Their Weathering Products. Edited by S.S. Augustithis. Theophrastus Publishers, Athens, p. 3, 1983.

Comans, R.N.J., H.A. van der Sloot and P.A. Bonouvrie. Speciatie van Contaminaten Tijdens Uitloging van AVI-Bodemas. Concept Eindrapport ECN-CX-93-XXX, April 1993.

Davis, J.A. and J.O. Leckie. Surface Ionization and Complexation at the Oxide/Water Interface. II. Surface Properties of Amorphous Iron Oxyhydroxide and Adsorption of Metal Ions. J. Colloid Interface Sci. 67, pp. 90-107, 1978.

Davis, J.A. and J.O. Leckie. Surface Ionization and Complexation at the Oxide/Water Interface. 3. Adsorption of Anions. J. Colloid Interface Sci. 74, pp. 32-43, 1980.

Davis, J.A. and D.B. Kent. Surface Complexation Modelling in Aqueous Geochemistry. In Mineral-Water Interface Geochemistry Edited by M.F. Hochella, Jr. and A.F. White. Mineralogical Society of America, Washington, D.C., p. 177, 1990.

de Groot, G.J., H.A. van der Sloot and J. Wijkstra. Leaching Characteristics of Hazardous Elements from Coal Fly Ash as a Function of the Acidity of the Contact Solution and the Liquid/Solid Ratio. In Edited by P.L. Côté and T.M. Gillian.In Environmental Aspects of Stabilization and Solidification of Hazardous and Radioactive Waste ASTM STP 1033, ASTM, Philadelphia, PA, pp. 170-183, 1987.

Drever, J.I. The Geochemistry of Natural Waters. Prentice-Hall, Englewood Cliffs, NJ, 1988.

Dudas, M.J. Long-Term Leachability of Selected Elements from Fly Ash. Environ. Sci. Technol. 15, pp. 840-843, 1981.

Eighmy, T.T., S.F. Bobowski, T.P. Ballestero and M.R. Collins. Theoretical and Applied Methods of Lead and Cadmium Stabilization in Combined Ash and Scrubber Residues. In Proceedings of the Second International Conference on Municipal Solid Waste Combustor Ash Utilization. Edited by W.H. Chesner and T.T. Eighmy. November 8-9, Arlington, VA, p. 275, 1990.

Evans, L.J. Chemistry of Metal Retention by Soil. Environ. Sci. Technol. 23, pp. 1046-1056, 1989.

Feitknecht, W. and P. Schindler. Solubility Constants of Metal Oxides, Metal Hydroxides and Metal Hydroxide Salts in Aqueous Solution. Butterworths, London, 1963.

Felmy, A.R., D.C. Girvin and E.A. Jenne. MINTEQ-A Computer Program for Calculating Aqueous Geochemical Equilibria. EPA-600/3-84-032, U.S. EPA, Athens, GA, 1984.

Fruchter, J.S., D. Rai and J.M. Zachara. Identification of Solubility-Controlling Solid Phases in a Large Fly Ash Field Lysimeter. Environ. Sci. Technol. 24, pp. 1173-1179, 1990.

Furuichi, R., N. Sato and G. Okamoto. Reactivity of Hydrous Ferric Oxide Containing Metallic Cations. Chimia 23, pp. 455-463, 1969.

Garrels, R.M. and C.L. Christ. Solutions, Minerals, and Equilibria. Harper and Row, New York, 1965.

Giovanoli, R. J.L. Schnoor, L. Sigg, W. Stumm and J. Zobrist. Chemical Weathering of Crystalline Rocks in the Catchment Area of Acidic Ticino Lakes, Switzerland. Clays Clay Min 36, pp. 521-529, 1989.

Grandstaff, D.E. Some Kinetics of Bronzite Orthopyroxene Dissolution. Geochim. Cosmochim. Acta 41, pp. 1097-1103, 1977.

Guggenheim, E.A. Applications of Statistical Mechanics, Clarendon Press, New York, 1966.

Harvie, C.E., N. Mϕller and J.H. Weare. "The Prediction of Mineral Solubilities in Natural Waters: The Na-K-Mg-Ca-H-Cl-SO_4-OH-HCO_3-CO_2-H_2O System to High Ionic Strengths at 25°C". Geochim. Cosmochim. Acta 48, pp. 735-751, 1984.

Harvie, C.E. and J.H. Weare. The Prediction of Mineral Solubilities in Natural Waters: the Na-K-Mg-Ca-Cl-SO_4-H_2O System from Zero to High Concentration at 25°C. Geochim. Cosmochim. Acta 44, p. 981-987, 1980.

Hayes, K.F. Equilibria, Spectroscopic and Kinetic Studies of Ion Adsorption at the Oxide Aqueous Interface. Ph.D. Dissertation, Stanford University, Palo Alto, CA, 1987.

Helgeson, H.C. Thermodynamics of Hydrothermal Systems at Elevated Temperatures and Pressures. Am. J. Sci. 267, pp. 729-804, 1969.

Hem, J.D. Equilibrium Chemistry of Iron in Groundwater. In Principles and Applications of Water Chemistry Edited by S.D. Faust and J.V. Hunter. John Wiley and Sons, New York, p. 625, 1967.

Hering, J.G. and W. Stumm. Oxidative and Reductive Dissolution of Minerals. In Mineral-Water Interface Geochemistry Edited by M.F. Hochella, Jr. and A.F. White. Mineralogical Society of America, Washington, D.C., p. 427, 1990.

Hsi, C.D. and D. Langmuir. Adsorption of Uranyl onto Ferric Oxyhydroxides: Application of the Surface Complexation Binding Site Models. Geochim. Cosmochim. Acta 49, pp. 1931-1941, 1985.

Kim, H.-T. and W.J. Frederick Jr. Evaluation of Pitzer Ion Internaction Parameters of Aqueous Electrolytes at 25°C.1. Single Salt Parameters. J. Chem. Eng. Data 33, pp. 177-184, 1988.

Kluge, G., H. Saalfeld and W. Dannecker. Untersuchungen des Langzeitverhaltens von Müllverbrennungsschlacken beim Einsatz im Strassenbau. Unweltforschungsplan des Bundesministers des Innern, Forschungsbericht Nr. 103 03 006. Berlin, 1980.

Krupka, K.M., R.L. Erikson, S.V. Mattigod, J.A. Schramke and C.E. Cowan. Thermochemical Data Used by the FASTCHEM Package. EPRI EA-5872, EPRI, Palo Alto, CA, 1988.

Kummert, R. and W. Stumm. The Surface Complexation of Organic Acids on Hydrous γ-Al_2O_3. J. Colloid Interface Sci. 75, pp. 373-385, 1980.

LaFlamme, B.D. and J.W. Murray. Solid/Solution Interaction: The Effect of Carbonate Alkalinity on Adsorbed Thorium. Geochim. Cosmochim. Acta 51, pp. 243-250, 1987.

Leckie, J.O. Coordination Chemistry at the Solid/Solution Interface. In Metal Speciation: Theory, Analysis and Application Edited by J.R. Kramer and H.E. Allen. Lewis Publishing, Chelsea, MI, 41, 1988.

Lindsay, W.J. Chemical Equilibria in Soils. J. Wiley and Sons, New York, 1979.

Millero, F.J. and D.R. Schreiber. Use of Ion Pairing Model to Estimate Activity Coefficients of the Ionic Components of Natural Waters. Am. J. Sci. 282, pp. 1508-1540, 1982.

Naumov, G.B., B.N. Ryzhenko and Khodakovsky. Handbook of Thermodynamic Data. US Geological Survey WRD-74-001. NTIS-PB-226 722/AS, Washington, D.C., 1974.

Nordstrom, D.K. and J.L. Munoz. Geochemical Thermodynamics. Blackwell Scientific Publications, Palo Alto, CA, 1986.

Nriagu, J.O. Lead Orthophosphates. IV. Formation and Stability in the Environment. Geochim. Cosmochim. Acta 38, pp. 887-898, 1974.

Oberste-Padtberg, R. and K. Schweden. Zur Freisetzung von Wasserstoff aus Mörteln mit MVA-Reststoffen. Wasser Luft Boden 34, pp. 61-62, 1990.

Pankow, J.F. Aquatic Chemistry Concepts. Lewis Publishers, Chelsea, MI,, 1991.

Pankow, J.F. and J.J Morgan. Kinetics for the Aquatic Environment. I. Environ. Sci. Technol 15, pp. 1155-1164, 1981a.

Pankow, J.F. and J.J. Morgan. Kinetics for the Aquatic Environment. II. Environ. Sci. Technol. 15, pp. 1306-1313, 1981b.

Parker, V.B., D.D. Wagman and W.H. Evans. Selected Values of Chemical Thermodynamic Properties. Tables for the Alkaline Earth Elements (Elements 92 through 97 in the Standard Order of Arrangement). U.S. National Bureau of Standards Technical Note 270-6, Gaithersburg, MD, 1971.

Parks, G.A. Surface Energy and Adsorption at Mineral/Water Interfaces: an Introduction. In Mineral-Water Interface Geochemistry Edited by M.F. Hochella Jr. and A.F. White. Mineralogical Society of American, Washington, D.C., p. 133, 1990.

Pitzer, K.S. Thermodynamics of Electrolytes. I. Theoretical Basis and General Equations. J. Phys. Chem. 77, pp. 268-277, 1973.

Pitzer, K.S. Theory Ion Interaction Approach. In Activity Coefficients in Electrolyte Solutions. Edited by R. Pytkowicz. CRC Press, Boca Raton, FL, p. 157, 1979.

Pitzer, K.S. Characteristics of Very Concentrated Aqueous Solutions. In Chemistry and Geochemistry of Solutions at High Temperatures and Pressures. Edited by D.T. Rickard and F.E. Wickman. Pergamon, Oxford, p. 249, 1981.

Pitzer, K.S. and L. Brewer. Thermodynamics, 2nd Edition, McGraw-Hill, New York, 1961.

Pitzer, K.S. and J.J. Kim. Thermodynamics of Electrolytes. IV. Activity and Osmotic Coefficients for Mixed Electrolytes. J. Am. Chem. Soc. 96, pp. 5701-5707, 1974.

Pitzer, K.S. and G. Mayorga. Thermodynamics of Electrolytes. II. Activity and Osmotic Coefficients for Strong Electrolytes with One or Both Ions Univalent. J. Phys. Chem. 77, pp. 2300-2308, 1973.

Pourbaix, M. Atlas of Electrochemical Equilibria. Pergammon Press, Oxford, 1966.

Pytkowicz, R.M. Equilibria, Nonequilibria, and Natural Waters, Vol. 1 and 2, John Wiley and Sons, New York, 1983.

Rai, D. Inorganic and Organic Constituents in Fossil Fuel Combustion Residues, Volume 1: A Critical Review. EPRI EA-5176, EPRI, Palo Alto, CA, 1987.

Rai, D. and J.M. Zachara. Chemical Attenuation Rates, Coefficients and Constants in Leachate Migration, Volume 1: A Critical Review. EPRI EA-3356, EPRI, Palo Alto, CA, 1984.

Robie, R.A., B.S. Hemingway and J.R. Fisher. Thermodynamic Properties of Minerals and Related Substances at 298.1K and 1 Bar Pressure and at Higher Temperatures. Geological Survey Bulletin No. 1452, U.S. Government Printing Office, Washington, D.C., 1978.

Robie, R.A., B.S. Hemingway and J.R. Fisher. Thermodynamic Properties of Minerals and Related Substances at 298.15°K and 1 bar Pressure and at Higher Temperatures. Geological Survey Bulletin 1452. U.S. Government Printing Office, Washington, D.C., 1979.

Rossotti, F. The Determination of Stability Constants. McGraw-Hill Co., Inc., New York, 1981.

Roy, W.R. and R.A. Griffin. Illinois Basin Coal Fly Ashes. 2. Equilibria Relationships and Qualitative Modelling of Ash-Water Reactions. Environ. Sci. Technol. 18, pp. 739-742, 1984.

Rubin, J. Transport of Reacting Solutes in Porous Media: Relations Between Mathematical Nature of Problem Formulation and Chemical Nature of Reactions. Water Resources Res. 19, pp. 1231-1252, 1983.

Scatchard, G. The Excess Free Energy and Related Properties of Solutions Containing Electrolytes. J. Am. Chem. Soc 90, pp. 3124-3127, 1968.

Schindler, P.W. and W. Stumm. The Surface Chemistry of Oxides, Hydroxides and Oxide Minerals. In Aquatic Surface Chemistry. Edited by W. Stumm. John Wiley and Sons, New York, p. 83, 1987.

Schnoor, J.L. Kinetics of Chemical Weathering: A Comparison of Laboratory and Field Weathering Rates. In Aquatic Chemical Kinetics: Reaction Rates of Processes in Natural Waters Edited by W. Stumm. John Wiley and Sons, New York, p. 475, 1990.

Schnoor, J.L. and W. Stumm. The Role of Chemical Weathering in the Neutralization of Acidic Deposition. Schweiz Z. Hydrol. 48, pp. 171-193, 1986.

Schott, J. and J.-C. Petit. New Evidence for the Mechanisms of Dissolution of Silicate Minerals. In Aquatic Surface Chemistry Edited by W. Stumm. John Wiley and Sons, New York, p. 293, 1987.

Schott, J., R.A. Berner and E.L. Sjöberg. Mechanism of Pyroxene and Amphibole Weathering. I. Experimental Studies of Iron-Free Minerals. Geochmi. Cosmochim. Acta 45, pp. 2123-2135, 1981.

Schumm, R.H., D.D. Wagman, S.M. Bailey, W.H. Evans and V.B. Parker. Selected Values of Chemical Thermodynamic Properties. Tables for the Lanthanide (Rare Earth) Elements (Elements 62 through 76) in the Standard Order of Arrangement. U.S. National Bureau of Standards Technical Note 270-7. U.S. Government Printing Office, Washington, D.C., 1973.

Schwertmann, U. and R.M. Taylor. Iron oxides. In Minerals in Soil Environments Edited by J.B. Dixon and S.B. Weed. Soil Science Society of America, Madison, WI, p. 145, 1977.

Sigg, L. Surface Chemical Aspects of the Distribution and Fate of Metal Ions in Lakes. In Aquatic Surface Chemistry Edited by W. Stumm. John Wiley and Sons, New York, p. 319, 1987.

Sigg, L. and W. Stumm. The Interactions of Anions and Weak Acids with the Hydrous Goethite (α-FeOOH) surface. Colloids Surf. 2, pp. 101-117, 1981.

Sillén, L.G. and A.E. Martell. Stability Constants of Metal-Ion Complexes. Supplement No. 1, Chemical Society, London, 1971.

Smith, R.M. and A.E. Martell. Critical Stability Constants. Plenum Press, New York, 1976.

Sposito, G. The Thermodynamics of Soil Solutions, Clarendon Press, Oxford, 1981.

Sposito, G. Chemical Models of Inorganic Pollutants in Soils. CRC Crit. Rev. Environ. Control 15, pp. 1-24, 1984.

Sposito, G. The Chemistry of Soils, Oxford University Press, N.Y., 1989.

Stämpfli, D. Final Report: Cement and Bottom Ash Chemistry (CABAC). ERG Report. UNH, Durham, NH, 1992.

Stämpfli, D., H. Belevi, R. Fontanive, and P. Baccini. Reactions of Bottom Ashes from MSW Incinerators and Construction Waste Samples with Water. EAWAG Project 3335, EAWAG, Dubendorf, Switzerland, 1990.

Stumm, W. and G. Furrer. The Dissolution of Oxides and Aluminum Silicates; Examples of Surface Coordination-Controlled Kinetics. In Aquatic Surface Chemistry, Edited by W. Stumm. John Wiley and Sons, New York, p. 197, 1987.

Stumm, W. and J.J. Morgan. Aquatic Chemistry. John Wiley and Sons, New York, 1981.

Stumm, W. and E. Weiland. Dissolution of Oxide and Silicate Minerals: Rates Depend on Surface Speciation. In Aquatic Chemical Kinetics: Reaction Rates of Processes in Natural Waters Edited by W. Stumm. John Wiley and Sons, New York, p. 367, 1990.

van der Wegen, G. Orienterend Onderzoek Naar Oorzaak Binding in een Monster AVI-Slakken. Rapportnumme, 91149, Intron, the Netherlands, 1991.

Verink, E.D. Simplified Procedure for Constructing Pourbaix Diagrams. J. Educational Modules Materials Sci. Engineer 1, pp. 535-560, 1979.

Wagman, D.D., W.H. Evans, V.B. Parker, I. Halow, S.M. Bailey and R.H. Schumm. Selected Values of Chemical Thermodynamic Properties. Tables for the First Thirty-Four Elements in the Standard Order of Arrangement. U.S. National Bureau of Standards Technical Note 270-3 U.S. Government Printing Office, Washington, D.C., 1968.

Wagman, D.D., W.H. Evans, V.B. Parker, I. Halow, S.M. Bailey and R.H. Schumm Selected Values of Chemical Thermodynamic Properties. Tables for Elements 35 through 53 in the Standard Order of Arrangement. U.S. National Bureau of Standards Technical Note 270-4 U.S. Government Printing Office, Washington, D.C., 1969.

Wagman, D.D., W.H. Evans, V.B. Parker, I. Halow, S.M. Bailey, R.H. Schumm and K.L. Churney. Selected Values of Chemical Thermodynamic Properties. Tables for Elements 54 through 61 in the Standard Order of Arrangement. U.S. National Bureau of Standards Technical Note 270-5 U.S. Government Printing Office, Washington, D.C., 1971.

Wagman, D.D., W.H. Evans, V.B. Parker, R.H. Schumm and R.L. Nuttall. Selected Values of Chemical Thermodynamic Properties. Compounds of Uranium, Protactinium, Thorium, Actinium, and the Alkali metals. U.S. National Bureau of Standards Technical Note 270-8 U.S. Government Printing Office, Washington, D.C., 1981.

Wagman, D.D., W.H. Evans, V.B. Parker, R.H. Schumm, I. Halow, S.M. Bailey, K.L. Churney and R.L. Nuttall. The NBS tables of Chemical Thermodynamic Properties. Selected Values for Inorganic and C_1 and C_2 Organic Substances in SI units. J. Phy. Chem. Ref. Data 11 (Supplement No. 2), pp. 1-392, 1982.

Warren, C.J. and M.J. Dudas. Weathering Processes in Relation to Leachate Properties of Alkaline Fly Ash. J. Environ. Qual. 13, pp. 530-538, 1984.

Warren, C.J. and M.J. Dudas. Formation of Secondary Minerals in Artificially Weathered Fly Ash. J. Environ. Qual. 14, pp. 405-410, 1985.

Warren, C.J. and M.J. Dudas. Mobilization and Attenuation of Trace Elements in Artificially Weathered Fly Ash. EPRI EA-4747, EPRI, Palo Alto, CA, 1986.

Wieland, E., B. Wehrli and W. Stumm. The Coordination Chemistry of Weathering: III a Generatlization on the Dissolution Rates of Minerals. Geochem. Cosmochim. Acta **52**: 1969-1981

Westall, J.C. and H. Hohl. A Comparison of Electrostatic Models for the Oxide/Solution Interface. Adv. Coll. Inter. Sci. 12, pp. 265-294, 1980.

Whitfield, M. An Improved Specific Interaction Model for Seawater at 25°C and 1 Atmosphere Total Pressure. Marine Chem. 3, pp. 197-213, 1975a.

Whitefield, M. The Extension of Chemical Models for Sea Water to Include Trace Components at 25°C and 1 Atmosphere Pressure. Geochim. Cosmochim. Acta 39, pp. 1545-1557, 1975b.

Wollast, R. and L. Chou. Kinetic Study of the Dissolution of Albite with Continuous Flow-Through Fluidized Bed Reactor. In The Chemistry of Weathering, Edited by J.I. Drever, NATO AI Series C 149, pp. 75-96, 1985.

Zachara, J.M., D.C. Girvin, R.C. Schmidt and C.T. Resch. Chromate Adsorption on Amorphous Iron Oxyhydroxide in the Presence of Major Groundwater Ions. Environ. Sci. Technol. 21, pp. 589-594, 1987.

Zachara, J.M. and G.P. Streile. Use of Batch and Column Methodologies to Assess Utility Waste Leaching and Subsurface Chemical Attenuation. EPRI EN-7313, EPRI, Palo Alto, CA, 1991.

Zevenbergen, C., J.P. Bradley, T. van der Wood, R.S. Brown, L.P. van Reeuwijk, and R.D. Schuiling. Weathering as a Process to Control the Release of Toxic Constituents from MSW Bottom Ash. In Geoconfine 93 Edited by M. Arnoud, M. Borres and B. Côme. A.A. Balkema, Rotterdam, p. 591, 1993.